Single-spin physics with weak bosons at RHIC

P.M. Nadolsky[1*] and C.-P. Yuan[2†]

[1] *Department of Physics,*

Southern Methodist University,

Dallas, Texas 75275-0175, U.S.A.

[2] *Department of Physics & Astronomy,*

Michigan State University,

East Lansing, Michigan 48824, U.S.A.

(Dated: 31st March, 2003)

Abstract

In order to measure spin-dependent parton distributions in production of $W^{\pm}$ bosons using the non-hermetic detectors of the Relativistic Heavy Ion Collider, an accurate model for distributions of charged leptons from the W boson decay is needed. We discuss the predictions for production and decay of the W bosons based on a calculation for resummation of large logarithmic contributions originating from multiple soft gluon radiation. We compare the predictions for the spin-dependent resummed cross sections with the corresponding next-to-leading order results. We show that the lepton-level asymmetries can be reliably predicted by the resummation calculation and directly compared to the experimental data. A program for the numerical analysis of such cross sections in γ^*, $W^{\pm}$, and Z^0 boson production is also presented.

PACS numbers: 12.38 Cy, 13.85.Qk , 13.88.+e

*Electronic address: nadolsky@mail.physics.smu.edu

†Electronic address: yuan@pa.msu.edu

I. INTRODUCTION

The measurement of longitudinal spin asymmetries in production of $W^{\pm}$ bosons at the Relativistic Heavy Ion Collider (RHIC) will provide an essential probe for spin-dependent quark distributions at high momentum scales Q^2 [1]. At a pp center-of-mass energy $\sqrt{s} = 500$ GeV, about 1.3×10^6 $W^+$and W^- bosons will be produced by the time the integrated luminosity reaches 800 pb^{-1}. Due to the parity violation in the $q\bar{q}W$ coupling, this process permits non-vanishing single-spin asymmetries $A_L(\xi)$, defined for any kinematical variable ξ as

$$A_L(\xi) \equiv \frac{\frac{d\sigma(p^{\rightarrow}p \rightarrow WX)}{d\xi} - \frac{d\sigma(p^{\leftarrow}p \rightarrow WX)}{d\xi}}{\frac{d\sigma(p^{\rightarrow}p \rightarrow WX)}{d\xi} + \frac{d\sigma(p^{\leftarrow}p \rightarrow WX)}{d\xi}}. \tag{1}$$

The Born-level expression for the asymmetry $A_L(y_W)$ with respect to the rapidity y_W of the W boson is particularly simple if the absolute value of y_W is large. In that case, the Born-level $A_L(y_W)$ reduces to the ratio $\Delta q(x)/q(x)$ of the polarized and unpolarized parton distribution functions [2–4]. Furthermore, $A_L(y_W)$ tests the flavor dependence of quark polarizations.

The original method for extracting the spin-dependent quark distributions out of the RHIC W boson data is based on the direct reconstruction of the asymmetry $A_L(y_W)$ [1, 5]. Unfortunately, such reconstruction is obstructed by specifics of the detection of $W^{\pm}$ bosons at RHIC. First, neither PHENIX [6] nor STAR [7] detector at RHIC is hermetic. Therefore, it is not possible at those detectors to monitor the energy balance in particle reactions, even in the transverse direction with respect to the beams. Due to the lack of information about the missing energy carried by the neutrino, the determination of y_W is in general ambiguous and depends on the assumptions about the dynamics of the process. Second, due to the correlation between the spins of the initial-state quarks and final-state leptons, the measured value of $A_L(y_W)$ is strongly sensitive to the experimental cuts imposed on the observed charged lepton. Hence, unless a theory calculation exists to reliably predict the distributions of the leptons from the W boson decay, the spin-dependent quark distribution functions cannot be determined with acceptable accuracy.

In weak boson production at the Fermilab Tevatron $p\bar{p}$ collider, the mass M_W of the W boson has been measured to a great precision [8, 9]. The information on M_W is extracted out of the lepton-level distributions $d\sigma/m_T$, $d\sigma/dp_{Te}$, or $d\sigma/dp_{T\nu}$, where

$p_{Te} \equiv |\mathbf{p}_{Te}|$ and $p_{T\nu} \equiv |\mathbf{p}_{T\nu}|$ are the transverse momenta of the electron and neutrino, and $m_T \equiv \sqrt{2p_{Te}p_{T\nu} - 2\mathbf{p}_{Te} \cdot \mathbf{p}_{T\nu}}$ is the transverse mass of the lepton pair. The value of M_W can be determined from the analysis of the position and shape of the Jacobian peaks in each of these three distributions. For most of the events contributing near the Jacobian peak, the transverse momentum q_T of the W boson is very small, of order of a few GeV. Therefore, at each order of the perturbative QCD calculation, there are large logarithmic contributions of the form $\alpha_S^n q_T^{-2} \ln^m(M_W^2/q_T^2)$, where $n = 1, 2, \ldots$ and $m = 0, 1, \ldots, 2n-1$. These large logarithmic contributions can be summed to all orders in α_S by applying the transverse momentum resummation formalism formulated in the impact parameter space by Collins, Soper, and Sterman (CSS) [10]. Without such a resummation calculation performed at the decay lepton level [11], it would not be possible to determine M_W from the experimental data. This is because at hadron colliders the longitudinal momentum of the neutrino from the W boson decay is not observed by the detectors; hence, the invariant mass of the W boson cannot be measured directly. Instead, the determination of the W boson mass relies on the analysis of the shape of the Jacobian peaks in the lepton-level distributions sensitive to q_T. Again, without a resummation calculation at the secondary lepton level, it would not be possible to predict the shape of these distributions accurately enough to determine M_W. We refer the reader to Ref. [11] for a detailed discussion of the phenomenology of the W boson physics at the Tevatron collider.

Similarly, at RHIC, a resummation calculation is needed to reliably predict the distribution of the secondary leptons from the W boson decay. As we already mentioned, the reason is the necessity to deduce spin-dependent parton luminosities based on the observation of the secondary charged lepton only. For RHIC purposes, the resummation calculation at the lepton level has to be modified to include the spin dependence, which has been performed in Ref. [12]. In this paper, we will apply the calculation in Ref. [12] to model single-spin asymmetries of W boson production in realistic RHIC conditions. We put the emphasis on the discussion of the asymmetries $A_L(y_\ell)$ and $A_L(p_{T\ell})$ for the distributions in the rapidity y_ℓ and transverse momentum $p_{T\ell}$ of the observed charged lepton. We will argue that these directly observed asymmetries provide a viable alternative to the commonly discussed asymmetry $A_L(y_W)$.

The paper is organized as follows. In Section II, we briefly summarize the resummation formalism used for this study. A next-to-leading order (NLO) calculation is also presented

for comparison to the resummation calculation. Since good understanding of spin-averaged cross sections is needed to derive polarized PDFs from the spin asymmetries, Section III discusses the uncertainties due to the imperfect knowledge of unpolarized parton distributions, as well as the potential for RHIC experiments to reduce these uncertainties. Section IV demonstrates that a correct model of multiple parton radiation is important to describe the differential distributions of the final-state leptons. We then employ the resummation calculation to realistically evaluate the feasibility of the reconstruction of the asymmetry $A_L(y_W)$ from the observed charged lepton data. Section V shows that the spin asymmetries for the distributions of the observed secondary leptons provide an attractive alternative to the asymmetry $A_L(y_W)$: they can be measured directly and discriminate efficiently between the different PDF sets. We also show that the RHIC experiments can explore the spin dependence of the nonperturbative contributions from the multiple parton radiation. The main findings of this paper are recapped in the conclusion.

II. THEORETICAL ESSENTIALS

The primary goal of this paper is to discuss production of $W^{\pm}$ bosons, which will be used at RHIC to obtain information about the longitudinally polarized parton distribution functions (PDFs) in the quark sector. Due to the unique feature of the maximal parity violation in the $Wq\bar{q}$ coupling, the parton-level cross sections for spin-dependent W boson production have pronounced single-spin asymmetries. This feature gives W boson production an edge on parity-conserving processes, in which non-trivial hadronic dynamics can be probed only through the measurement of more complex double-spin asymmetries.

Denote the unpolarized distribution of a parton a in a nucleon A as $f_{a/A}(\xi, \mu_F)$ and the longitudinally polarized distribution of a in the nucleon A as $\Delta f_{a/A}(\xi, \mu_F)$. Then,

$$f_{a/A}(\xi, \mu_F) \equiv f_{+/+}(\xi, \mu_F) + f_{-/+}(\xi, \mu_F), \tag{2}$$

$$\Delta f_{a/A}(\xi, \mu_F) \equiv f_{+/+}(\xi, \mu_F) - f_{-/+}(\xi, \mu_F), \tag{3}$$

where $f_{h_a/h_A}(\xi_a, \mu_F)$ is a helicity-dependent parton distribution function, i.e., a probability of finding a parton a with the momentum $p_a^\mu = \xi_a p_A^\mu$ and helicity h_a in a hadron A with the momentum p_A^μ and helicity h_A. The PDFs depend on the factorization scale μ_F, which in our calculation is assumed to coincide with the QCD renormalization scale. To find the

polarized PDFs from an experiment with one longitudinally polarized beam, one measures the unpolarized cross section,

$$\frac{d\sigma}{d\xi} = \frac{1}{2}\left(\frac{d\sigma(p^{\rightarrow}p \to WX)}{d\xi} + \frac{d\sigma(p^{\leftarrow}p \to WX)}{d\xi}\right), \tag{4}$$

as well as the single-spin cross section,

$$\frac{d\Delta_L\sigma}{d\xi} = \frac{1}{2}\left(\frac{d\sigma(p^{\rightarrow}p \to WX)}{d\xi} - \frac{d\sigma(p^{\leftarrow}p \to WX)}{d\xi}\right). \tag{5}$$

Here ξ denotes any kinematic variable, such as the rapidity y_W of the W boson. The single-spin asymmetry is defined as

$$A_L(\xi) \equiv \frac{d\Delta_L\sigma/d\xi}{d\sigma/d\xi}. \tag{6}$$

In Ref. [12], we presented fully differential unpolarized cross sections $d\sigma/d\xi$, single-spin cross sections $d\Delta_L\sigma/d\xi$, and double-spin cross sections $d\Delta_{LL}\sigma/d\xi$ for production and decay of γ^*,$W^{\pm}$, and Z^0 bosons. To reliably predict the rate at any point of the momentum phase space, these cross sections include the all-order sum of large soft and collinear logarithms, which dominate at small transverse momentum q_T of the vector boson. This all-order sum is combined, without double counting, with the finite-order $\mathcal{O}(\alpha_S)$ cross section, which dominates at large q_T. The single-spin resummed cross sections in the narrow width approximation were first obtained in Ref. [13]. The main result of Ref. [12] is the (more involved) derivation of the resummed cross sections that also accounts for the decay of the vector bosons and angular distributions of the final-state leptons. Our result was derived in the $\overline{MS}$ factorization scheme [14–16]; therefore, it is fully compatible with the $\overline{MS}$ parton distributions.

The resummed cross sections from Ref. [12] are implemented in the numerical resummation program LEGACY and Monte-Carlo integration program RHICBOS,[1] which were used to produce the results discussed in this paper. LEGACY is a C++/Fortran program that quickly and accurately generates the resummed cross sections on a grid of points in the kinematical phase space. RHICBOS reads in the cross section grids, performs their multi-dimensional integration, and produces the output that is optimized for RHIC specifics. Since the finite-order cross section is characterized by a smaller theoretical uncertainty at $q_T \gtrsim Q$,

[1] The Fortran code and input grids for RHICBOS can be downloaded from http://hep.pa.msu.edu/~nadolsky/RhicBos/.

RHICBOS switches from the resummed cross section ($W+Y$) to the finite-order cross section at the point where the resummation cross section becomes smaller than the finite-order cross section at q_T above the position of the maximum in $d\sigma/dq_T$. To compare the resummation calculation to the finite-order approach, we have also calculated the finite-order $\mathcal{O}(\alpha_S)$ cross section (next-to-leading order, or NLO, cross section) with the help of a phase space slicing method. This method introduces a separation transverse momentum scale q_T^{sep}, below which the integral of $d\sigma/dq_T^2$ over the region $0 \leq q_T^2 \leq (q_T^{sep})^2$ is calculated analytically, using the small-q_T approximation in Eq. (78) of Ref. [12]. The integral over the region $q_T^2 \geq (q_T^{sep})^2$ is integrated numerically using the exact $\mathcal{O}(\alpha_S)$ cross section. As we will show later, in the NLO approach, predictions for several important distributions depend strongly on the value of the auxiliary parameter q_T^{sep}, so that the resummed cross sections must be used in order to model those distributions. Some other distributions, such as $d\sigma/dQ^2$, are not sensitive to q_T^{sep} (up to higher-order corrections), so that the resummation and NLO calculations give close results for such distributions.

The electroweak parameters in this paper were obtained in the on-shell scheme according to the procedure described in Section II.B of Ref. [12] for the Fermi constant $G_F = 1.16639 \times 10^{-5}$ GeV^{-2}, W boson mass $M_W = 80.419$ GeV, and Z^0 boson mass $M_Z = 91.187$ GeV. The width Γ_W of the W boson was evaluated as $\Gamma_W = 3G_F M_W^3/(2\pi\sqrt{2})$. The finite-order and asymptotic cross sections were calculated for the QCD factorization scale $\mu_F = Q$. The resummed cross section (see Eqs. (79) and (80) in Ref. [12]) was calculated for the canonical values of the scale parameters, $C_1 = C_3 = 2e^{-\gamma_E}$, where $\gamma_E \approx 0.577$ is the Euler constant, and $C_2 = 1$. Unless stated otherwise, the nonperturbative Sudakov factor in the resummed cross sections was evaluated by using the recent Gaussian parametrization [17] derived from the global analysis of transverse momentum distributions in unpolarized vector boson production. The projected statistical errors δA_L in the measurement of the single-spin asymmetries were estimated according to Eq. (13) in Ref. [1]:

$$\delta A_L = \sqrt{\frac{1}{NP^2} - \frac{1}{N}A_L^2}, \tag{7}$$

where $N = \mathcal{L}\sigma$ is the number of the events for the given luminosity $\mathcal{L}$ and cross section σ. Unless stated otherwise, the assumed integrated luminosity is $\mathcal{L} = 800$ pb^{-1}, and polarization P of the beam A is 70%.

III. PHYSICS POTENTIAL IN UNPOLARIZED pp COLLISIONS

To extract the single-spin cross section $d\Delta_L\sigma/d\xi$ from the single-spin asymmetry $A_L(\xi)$, the spin-averaged cross sections $d\sigma/d\xi$ must be known well. Obviously, the uncertainty in the knowledge of $d\sigma/d\xi$ must be small enough as compared to the targeted uncertainty in the measurement of $d\Delta_L\sigma/d\xi$. Therefore, an interesting question is: how well do we currently know the unpolarized cross sections at RHIC energies, and how important is their measurement in the upcoming RHIC experiments? The goal of this section is to argue that at present the uncertainties in the unpolarized cross sections at RHIC are sizeable; to reliably predict the unpolarized rate, these uncertainties must be reduced by dedicated RHIC measurements.

Table I lists the unpolarized cross sections and event rates for the processes $pp \to (W^\pm \to \ell\nu_\ell)X$ and $pp \to (Z^0 \to \ell\bar{\ell})X$ at RHIC for various values of center-of-mass energies $\sqrt{s}$ and integrated luminosities $\mathcal{L}$. The cross sections were derived at NLO using the updated CTEQ6 parton distribution functions [18, 19]. The cross sections σ are calculated using the best-fit PDF parametrization CTEQ6M. The uncertainty $\delta\sigma_{PDF}$ in the cross section σ is generated by the uncertainty in the unpolarized parton luminosities, which are themselves phenomenological functions known with a finite precision. This uncertainty is evaluated with the help of the Hessian matrix analysis employed in Ref. [18]. Specifically, $\delta\sigma_{PDF}$ corresponds to the maximal variation of σ for all possible PDF parametrizations lying in the acceptable range of χ^2. According to Table I, the relative PDF uncertainties are of order 25% at $\sqrt{s} = 200$ GeV and $7-10\%$ at $\sqrt{s} = 500$ GeV. These are the errors that exist prior to the measurements at RHIC.

The above PDF uncertainties are large because W and Z boson production at the pp collider RHIC probes the sea quark distributions (primarily $\bar{u}(x)$ and $\bar{d}(x)$) at $x \gtrsim 0.1$. For instance, the major part of W boson events occurs in the central-rapidity region $y_W \approx 0$ and corresponds to the Born-level momentum fractions $x = Q/\sqrt{s}$ close to 0.4 and 0.16 at $\sqrt{s} = 200$ GeV and $\sqrt{s} = 500$ GeV, respectively. At such x the sea quark PDFs are not as constrained by the existing (mostly DIS) data, which better determine the valence-dominated distributions $u(x)$ and $d(x)$. Therefore, RHIC provides the information that is complementary to the DIS experiments at HERA and collider experiments at the $p\bar{p}$ collider Tevatron.

This point is illustrated by Fig. 1, which shows the relative PDF uncertainty $\delta\sigma_{PDF}/\sigma$ in $W^{\pm}$ and Z^0 boson production at various existing colliders. To compare the potential of pp and $p\bar{p}$ colliders of the same center-of-mass energy, this figure also shows the PDF uncertainties at fictitious $p\bar{p}$ colliders with $\sqrt{s} = 200$ and 500 GeV. According to the figure, the PDF uncertainties at RHIC substantially exceed the uncertainties at the Tevatron and LHC. They are also up to 2.5 times larger than the PDF uncertainties at the fictitious $p\bar{p}$ colliders of RHIC energies. The PDF uncertainty is the largest in W^- boson production at RHIC, which is sensitive primarily to the $d\bar{u}$ combination of the parton distributions.

On the other hand, for the planned integrated luminosities, RHIC will measure the spin-averaged rates with better accuracy, particularly in W^+ boson production. At $\sqrt{s} = 500$ GeV and $\mathcal{L} = 800$ pb^{-1}, the 2σ relative statistical errors ($2N^{-1/2}$) in the rate are 0.6%, 1.2%, and 2% in W^+, W^-, and Z^0 boson production, respectively. At $\sqrt{s} = 200$ GeV and $\mathcal{L} = 320$ pb^{-1}, the respective errors are 10%, 18%, and 44%. We see that the projected statistical errors in W boson production are smaller than the current PDF errors. Therefore, we conclude that the measurement of the spin-averaged cross sections at RHIC will drastically reduce the uncertainty in the unpolarized parton distributions in the probed region of x. We emphasize that the measurement of the spin-averaged cross sections should be an important part of the RHIC physics program, since it complements information about the unpolarized PDFs from the other colliders and reduces systematic uncertainties in the measured polarized cross sections.

IV. RECONSTRUCTION OF SPIN ASYMMETRIES FROM RHIC DATA

A. Impact of multiple parton radiation on differential distributions

To extract useful information from the raw data in W boson production, it is necessary to unfold the kinematical acceptance of the signal events, which can only be reliably predicted by a resummation calculation, similar to what has been done for the W boson physics at the Tevatron [11]. The correct lepton-level calculation is even more indispensable given that RHIC cannot register the transverse energy carried by the decay neutrino.

For definiteness, let us concentrate on the production of W^+ bosons. Of course, all conclusions in this section hold for W^- boson production as well. Fig. 2 shows the transverse

momentum distributions of the W^+ boson and charged lepton from its decay, as predicted by the resummation package LEGACY-RHICBOS. Here and after, the numerical results correspond to the c.m. energy $\sqrt{s} = 500$ GeV and integrated luminosity $\mathcal{L} = 800$ pb^{-1}. It is evident that most of the W bosons are produced with small, but non-zero transverse momenta. Such non-zero q_T is acquired through radiation of soft and collinear partons, which cannot be approximated by finite-order perturbative calculations. In order to obtain reliable predictions for differential cross sections, dominant logarithmic terms $\alpha_S^n \ln^m (q_T^2/Q^2)$ (where $0 \leq m \leq 2n-1$) associated with such radiation should be summed through all orders of the perturbative series.

Furthermore, consider the distribution $d\sigma/dp_{T\ell}$ in Fig. 2(b). If the transverse momentum q_T and width Γ_W of the W boson were negligible (as in the Born-level calculation), $d\sigma/dp_{T\ell}$ would show a singular Jacobian peak exactly at $p_{T\ell} = M_W/2$. The smearing of the Jacobian peak in Fig. 2(b) is due to the multiple soft gluon radiation and non-zero width of the W boson. The example of $d\sigma/dp_{T\ell}$ illustrates that multiple parton radiation and heavy boson decay may drastically alter the Born-level predictions. The resummation effects are important if the distribution is sensitive to q_T directly (as $d\sigma/dp_{T\ell}$), or if the phase space is constrained in a region with slower convergence of perturbation theory (as $d\sigma/dy_\ell$ at large $|y_\ell|$). In the remainder of this section, we utilize this accurate calculation to evaluate feasibility of the measurement of the boson-level asymmetry $A_L(y_W)$, which is commonly discussed in literature as the most convenient observable to probe polarized sea quark distributions. Many aspects of our discussion are based on the analysis of two-variable distributions $d^2\sigma/(dp_{T\ell}dy_\ell)$ in the transverse momentum and rapidity of the observed charged lepton. These distributions for the unpolarized and single-spin W^+ and W^- boson production are shown in Fig. 3.

B. W boson rapidity at the Born level

Consider the Born-level expression for the following asymmetry in W^+ boson production induced by the up quark and down antiquark via $u\bar{d} \to W^+ \to \ell^+\nu_\ell$:

$$\begin{aligned} A_L(y_W, \theta^*) &\equiv \frac{d\Delta_L\sigma/(dQ^2 dy_W d\cos\theta^*)}{d\sigma/(dQ^2 dy_W d\cos\theta^*)} \\ &= \frac{-\Delta u(x_A)\bar{d}(x_B)(1+\cos\theta^*)^2 + \Delta\bar{d}(x_A)u(x_B)(1-\cos\theta^*)^2}{u(x_A)\bar{d}(x_B)(1+\cos\theta^*)^2 + \bar{d}(x_A)u(x_B)(1-\cos\theta^*)^2}. \end{aligned} \tag{8}$$

Here $x_{A,B} \equiv (Q/\sqrt{s})e^{\pm y_W}$, and θ^* is the polar angle of the charged lepton in the rest frame of the W boson, with the z axis pointing in the moving direction of the polarized proton beam. The single-spin asymmetry $A_L(y_W)$ in the rapidity of the W boson can be obtained from Eq. (8) by integrating $\cos\theta^*$ out, i.e., integrating over the moving direction of ℓ^+ and ν_ℓ:

$$A_L(y_W) \;=\; \frac{\int_{-1}^{1} \frac{d\Delta_L\sigma}{dQ^2 dy_W d\cos\theta^*} d\cos\theta^*}{\int_{-1}^{1} \frac{d\sigma}{dQ^2 dy_W d\cos\theta^*} d\cos\theta^*} = \frac{-\Delta u(x_A)\bar{d}(x_B) + \Delta\bar{d}(x_A)u(x_B)}{u(x_A)\bar{d}(x_B) + \bar{d}(x_A)u(x_B)}. \tag{9}$$

The resulting expression for $A_L(y_W)$ is commonly discussed in literature as an example of a simple observable, which is straightforwardly sensitive to $\Delta u(x)$ and $\Delta\bar{d}(x)$. Similarly, the Born-level asymmetry $A_L(y_W)$ in W^- boson production is straightforwardly sensitive to $\Delta\bar{u}(x)$ and $\Delta d(x)$. It has been also argued in Ref. [22] that $\mathcal{O}(\alpha_S)$ corrections cancel to a good degree between the numerator and denominator of $A_L(y_W)$. Unfortunately, as we will now demonstrate, the measurement of $A_L(y_W)$ is obstructed by the effects of W boson decay and the limited detector acceptance, which seriously complicate both the reconstruction of y_W and determination of $A_L(y_W)$ from the observed data.

Let us first discuss the determination of the rapidity of the W boson. Given that neither of the two RHIC detectors measures the missing energy, the four-momentum of the W boson cannot be deduced from the momenta of its decay products. Therefore the rapidity of the W boson cannot be measured directly.

Despite the impossibility to measure y_W in general, it has been proposed [1, 5] to statistically *choose* the correct y_W in a certain kinematical region based on several assumptions about the QCD dynamics of the process. Let us outline the main idea of this method.

Denote the rapidity and transverse momentum of the lepton in the lab frame as y_ℓ and $p_{T\ell}$, respectively. Similarly, denote the corresponding variables in the rest frame of the W boson as y'_ℓ and $p'_{T\ell}$, respectively. In the naive Born approximation, the W bosons have zero width ($Q = M_W$) and zero transverse momentum ($q_T = 0$). Therefore, the lepton variables in the different reference frames are related as

$$y_\ell \;=\; y'_\ell + y_W, \tag{10}$$

$$p_{T\ell} \;=\; q_T + p'_{T\ell} \;\;=\;\; p'_{T\ell}, \tag{11}$$

$$\qquad\qquad\quad \uparrow$$

$$\qquad\qquad q_T = 0$$

where y'_ℓ and $p'_{T\ell}$ are the functions of the polar angle θ^* of the lepton in the W boson rest frame:

$$y'_\ell = \frac{1}{2}\ln\frac{1+\cos\theta^*}{1-\cos\theta^*}, \tag{12}$$

$$p'_{T\ell} = \frac{Q}{2}\sin\theta^* \quad \underset{Q=M_W}{\overset{\uparrow}{=}} \quad \frac{M_W}{2}\sin\theta^*. \tag{13}$$

The comments below the equations show the assumptions involved in obtaining the rightmost expressions in Eqs. (11) and (13).

For a given set of y_ℓ and $p_{T\ell}$, Eqs. (10)-(13) imply two solutions y_+ and y_- (corresponding to θ^* and $\pi-\theta^*$) for y_W. One of them can be correctly chosen if the magnitude of the rapidity y_ℓ of the charged lepton is large (i.e., if the lepton is observed in the forward or backward rapidity region). In these special regions, one of the two solutions for y_W can always be discarded, because it takes a value outside of the allowed rapidity range of the collider. In other words, the chosen solution is the one with the smaller magnitude. However, in reality, q_T never vanishes, as predicted by the resummation calculation (see Fig. 2(a)). Similarly, Γ_W is not zero. Therefore, the above approximation never holds exactly, and the size of the error is determined by the difference between the Born-level and exact dynamics.

By comparing the leading order, NLO, and resummation calculations, we have found that the approximation holds reasonably well when $q_T \ll M_W$, $p'_{T\ell} \approx p_{T\ell}$, and y_ℓ is large. This point is illustrated in Fig. 4, which shows the statistically averaged differences $\langle(|y_\pm - y_W|)\sigma\rangle/\langle\sigma\rangle$ between the exact y_W and each of the two solutions $y_\pm$ in the two-dimensional plane of y_ℓ and $p_{T\ell}$, predicted by the resummation calculation. It can be seen that the difference is small for one of the solutions in the respective region $y_\ell \gtrsim 1$ or $y_\ell \lesssim -1$, and $p_{T\ell} \lesssim 25-30$ GeV. At the same time, the difference is unacceptably large for the other solution. Correspondingly, in each special region the distribution in the correct solution y_+ or y_- closely reproduces the distribution in true y_W. For example, Fig. 5 shows that the distributions $d\sigma/dy_-$ agrees well with the distribution $d\sigma/dy_W$ in the region 10 GeV $\leq p_{T\ell} \leq 30$ GeV and $1.2 \leq y_\ell \leq 2.4$.

Except for the special regions in Fig. 4, the approximate solutions $y_\pm$ do not agree well with the exact y_W. An important feature to note is that in the special regions the event rate is small. As shown in Fig. 3, most of the event rate comes from $p_{T\ell} \sim M_W/2$ and $y_\ell \sim 0$. Furthermore, the magnitude of the error in y_W depends on the shape of the cross section,

which, of course, is unknown *a priori* in the polarized case.

C. Distortion effects on $A_L(y_W)$

Let us now turn to another problem in the measurement of $A_L(y_W)$: distortions in the deduced shape of $A_L(y_W)$ due the experimental cuts. To obtain $A_L(y_W)$, the experimental cross sections have to be integrated over all possible directions of the lepton motion, i.e., over $\cos\theta^*$ in the interval $-1 \leq \cos\theta^* \leq 1$ (see Eq. (9) for an example of such integration in the Born-level analysis). Unfortunately, the acceptance of RHIC detectors does not permit such integration, so that the resulting asymmetry has the residual dependence on the acceptance range in $\cos\theta_*$ and does not agree with the true asymmetry $A_L(y_W)$.

Indeed, $\cos\theta^*$ is related to the rapidity of the lepton y_ℓ via Eqs. (10) and (12):

$$y_\ell = y_W + \frac{1}{2}\ln\frac{1+\cos\theta^*}{1-\cos\theta^*}.$$

Therefore, the restrictions on the range of y_ℓ reduce the range of integration over $\cos\theta^*$. Specifically, the PHENIX muon detectors are able to detect a muon if the muon rapidity y_μ and azimuthal angle ϕ_μ satisfy $1.2 \leq |y_\mu| \leq 2.4$ and $0 \leq \phi_\mu \leq 2\pi$. The PHENIX electromagnetic calorimeter can register electrons with $|y_e| \leq 0.35$ and $0 \leq \phi_e \leq \pi$. The STAR detector registers electrons in the barrel electromagnetic calorimeter that covers $|y_e| \leq 1.0$ and $0 \leq \phi_e \leq 2\pi$. In addition, a selection cut $p_{T\ell} \gtrsim 10 - 20$ GeV is expected to be imposed on the charged leptons to suppress background contributions, which also constrains $\sin\theta^*$ through Eqs. (11) and (13).

The effect of the above cuts is demonstrated in Fig. 6, which shows the single-spin asymmetry in W^+ boson production calculated without constraints on y_ℓ and $p_{T\ell}$ (solid line), as well as with the constraints $1.2 < |y_\ell| < 2.4$, $p_{T\ell} > 20$ GeV (circles) and $|y_\ell| < 1$, $p_{T\ell} > 20$ GeV (boxes). The results shown here are derived using the resummation calculation.[2] According to the figure, there is a substantial difference between the asymmetries calculated with and without experimental cuts. This difference arises due to the different dependence of

[2] For the asymmetries $A_L(y_W)$, the resummation and NLO calculations give close predictions (within one estimated statistical error δA_L), even though these calculations predict quite different shapes for the unpolarized and polarized differential cross sections.

the unpolarized and polarized cross sections on angular distributions of the charged leptons, which affects the asymmetry because $\cos\theta^*$ is not integrated out completely.

The findings in this section can be summarized as follows. The extraction of $A_L(y_W)$ from RHIC data is not an easy task, because (a) the direct measurement of y_W is impossible, and (b) the reconstructed $A_L(y_W)$ is distorted by the experimental acceptance cuts. In particular, the two-fold ambiguity in the determination of y_W is unavoidable at $y_\ell \sim 0$ and $p_{T\ell} \sim M_W/2$, i.e., in the region with the largest cross section. To take the full advantage of the large event rate at RHIC, we ought to seek an alternative to $A_L(y_W)$, which is free of the complications discussed above. In the next section, we turn our attention to the spin asymmetries of the lepton-level cross sections $d\sigma/dy_\ell$ and $d\sigma/dp_{T\ell}$, which may serve as such alternative observables. Based on the resummation calculation, we analyze the sensitivity of the lepton-level asymmetries to the choice of the experimental cuts. We also present theoretical predictions for various PDF sets.

V. SINGLE-SPIN ASYMMETRIES AT THE LEPTON LEVEL

A. Impact of the cuts and soft radiation on lepton-level cross sections

Let us first separately discuss the unpolarized and polarized cross sections. To study the detector effects on the shape of various distributions, we will compare the cross sections for the kinematical acceptance of PHENIX and STAR detectors, as well as cross sections without any kinematical cuts. We also compare the resummation calculation to the NLO calculation, with the latter performed in the phase space slicing method for the separation parameter $q_T^{sep} = 1.6$ GeV. We concentrate on the distributions $d\sigma/dp_{T\ell}$, where the differences between the resummed and NLO predictions are the most visible.

Fig. 7 presents the distribution $d\sigma/p_{T\ell}$ for the positively charged leptons from the decay of W^+ bosons. The shape of the NLO cross sections (dashed curves) for $p_{T\ell}$ around and above $M_W/2$ (i.e., the Jacobian peak) is strongly affected by the arbitrary parameter q_T^{sep} employed in this calculation. Hence, the only reliable predictions for this part of the phase space are given by the resummed cross sections (shown as the solid curves). For smaller $p_{T\ell}$, the resummation calculation agrees with the NLO calculation, because it is formulated to match the NLO calculation in the region where the multiple gluon emission is not important.

Furthermore, without any kinematic cuts, the integrated rate of the resummation calculation agrees with that of the NLO calculation to a percent level. As shown in Fig. 7(b), the selection of the leptons in the large rapidity region distorts the shape of the $p_{T\ell}$ distribution by suppressing the contributions near the Jacobian peak. On the other hand, the selection of the central-rapidity region $|y_e| < 1.0$ (cf. Fig. 7(c)) suppresses the contributions with $p_{T\ell} \lesssim 10$ GeV. Both features can be understood from the shape of the differential distribution $d^2\sigma/(dp_{T\ell}dy_\ell)$ given in Fig. 3(a). According to this figure, the small (large) rapidity $|y_\ell|$ statistically corresponds to the large (small) transverse momentum $p_{T\ell}$.

As a pp collider, RHIC produces different numbers of W^- and W^+ bosons because of different parton luminosities. Due to the different rapidity distributions for W^+ and W^- bosons, the rapidity cuts have a different effect on $d\sigma/dp_{T\ell}$ in these processes. Fig. 8 shows the distributions $d\sigma/dp_{T\ell}$ in the process $pp \to (W^- \to \ell^-\bar{\nu}_\ell)X$. We find that the shape of the distributions without cuts shown in Fig. 8(a) is very close to the shape of the corresponding distribution in Fig. 7(a), even though the overall normalizations are obviously different. On the other hand, the shapes do not coincide in the presence of the cuts, in particular in the case of the PHENIX selection cuts shown in Figs. 7(b) and 8(b).

The $p_{T\ell}$ distributions in the single-spin W^+ boson production are shown in Fig. 9. The cross sections $d\Delta_L\sigma/dp_{T\ell}$ in W^+ boson production are negative, because the charged weak coupling is purely left-handed, and the dominant polarized PDF $\Delta u(x)$ is positive in the RHIC range of x. Again, we see that the NLO calculation cannot reliably predict the distribution of $p_{T\ell}$ around and above $M_W/2$. For the PHENIX kinematics, cf. Fig. 9(b), a sharper peak is developed in the distribution of $p_{T\ell}$ around $M_W/2$ as compared to the unpolarized case, cf. Fig. 7(b). The different shape is caused by the different rapidity dependence in the unpolarized and single-spin cases, as shown in Figs. 3(a) and 3(c). Finally, the distribution $d\sigma/dp_{T\ell}$ for the charged leptons ℓ^- in the W^- events is shown in Fig. 10.

For the rapidity distributions $d\sigma/dy_\ell$ without imposed cuts on $p_{T\ell}$, the NLO and resummed cross sections are close to one another, in accordance with the cancellation of soft contributions in sufficiently inclusive observables. However, according to the discussion above, the resummation and NLO predictions for $d\sigma/dy_\ell$ can be very different if cuts on $p_{T\ell}$ are imposed.

B. Single-spin asymmetries

We now turn our attention to the single-spin asymmetry. Since the only straightforward signature of the W bosons at RHIC is the observation of the secondary charged leptons, it is important to understand these asymmetries at the lepton level. In Figs. 11 and 12, we show the lepton-level asymmetries $A_L(y_\ell)$ in the W^+ and W^- events, respectively, for various cuts on $p_{T\ell}$. In these figures, the positive rapidity direction is in the moving direction of the polarized proton beam. Similarly, Figs. 13 and 14 show the asymmetries $A_L(p_{T\ell})$ for various cuts on y_ℓ. All asymmetries are derived using the Gehrmann-Stirling PDF sets A and B [23] and GRSV-2000 valence-like PDF set [21] in the resummation calculation. We found by experimenting with other available PDF sets in Refs. [21, 23, 24] that the shown graphs characterize well the possible span in the asymmetry due to the different polarized PDF parametrizations. The projected statistical errors are estimated according to Eq. (7) for the bin sizes shown in the figure.

According to the figures, the lepton-level asymmetries can be accurately measured for both W^+ and W^- bosons. These directly observed asymmetries can efficiently discriminate between different PDF sets; hence, they provide a viable alternative to the less accessible asymmetry $A_L(y_W)$. For both $W^+$and W^- boson samples (cf. Figs. 11 and 12), the power to discriminate between different PDF sets is larger in the region of the positive rapidity y_ℓ, especially for the W^- boson data. It is interesting to observe that, in different ranges of y_ℓ, the largest variations due to the choice of the PDFs appear in different ranges of $p_{T\ell}$. In W^+ boson production, the largest variation in the asymmetries $A_L(p_{T\ell})$ is concentrated at $p_{T\ell} \gtrsim 30 - 40$ GeV in the backward rapidity region $y_\ell < 0$ (Fig. 13(a) and (b)) and at $p_{T\ell} \lesssim 30 - 40$ GeV in the forward rapidity region $y_\ell > 0$ (Fig. 13(c) and 13(d)). In W^- boson production the largest variation is observed for very forward leptons, $1.2 < y_\ell < 2.4$ (Fig. 14(d)). If an additional condition $p_{T\ell} > 20$ GeV is imposed, other regions of y_ℓ (cf. Fig. 14(a)-14(c)) show a smaller sensitivity to different PDF sets.

During the first years of RHIC spin program, it may not be possible to distinguish between the positively and negatively charged leptons from the W boson decay, particularly before the solenoid field of the STAR detector is fully operational. It is therefore interesting to examine the possibility of measuring the single-spin asymmetries in the combined sample of W^+ and W^- bosons, without distinguishing between charged leptons and anti-leptons. Such

asymmetries are shown in Figs. 15 and 16. Since there are about three W^+ bosons produced per each W^- boson, these asymmetries are close to the W^+ boson asymmetries shown in Figs. 11 and 12. Therefore, these asymmetries will be able to distinguish between different PDF sets for a sufficiently high number of events.[3] However, they cannot completely replace the single-spin asymmetries for independent W^+ and W^- boson samples, which have better discriminating power and allow us to distinguish between contributions of different parton flavors.

C. Nonperturbative contribution

As was discussed above, the transverse momentum distributions for vector bosons are affected by the soft and collinear radiation, which can be described only by means of all-order resummation. In addition, the distributions at very small q_T are sensitive to nonperturbative contributions characterized by large impact parameters $b \gtrsim 1$ GeV^{-1}. As a result, the shape of the lepton-level distribution $d\sigma/dp_{T\ell}$ around its peak at about $p_{T\ell} = M_W/2$ is affected by both perturbative and nonperturbative QCD radiation, in addition to the nonzero width of the W boson. While the perturbative soft and collinear contributions can be calculated order-by-order in the resummation formalism, the nonperturbative contributions (associated with the nonperturbative transverse motion of partons inside the proton) can only be approximated by phenomenological parametrizations. In particular, based on the factorization properties of the resummed cross sections, one can hypothesize a simple relationship between the nonperturbative Sudakov factors in the unpolarized, single-spin, and double-spin vector boson production:

$$S_{NP}|_{single-spin} = \frac{1}{2}\left(S_{NP}|_{unpolarized} + S_{NP}|_{double-spin} \right). \tag{14}$$

Furthermore, S_{NP} is usually assumed to be independent of the type of the electroweak hard probe, so that it is the same in γ^*, W, and Z boson production. If the relationship (14) for the spin dependence of S_{NP} indeed holds in nature, the nonperturbative contributions in single-spin W boson production can be determined unambiguously once the parametrizations of

[3] Of course, the projected error bars in Figs. 15 and 16 (evaluated for $\mathcal{L} = 800$ pb^{-1}) will have to be adjusted to agree with the actual integrated luminosity at the time of the measurement.

S_{NP} on the right-hand side of Eq. (14) are available, e.g., from the global analysis of the distributions $d\sigma/dq_T$ in the unpolarized and double-spin γ^* or Z^0 production.

It is well known from the unpolarized studies (see, e.g., Refs. [10, 25, 26]) that the importance of the nonperturbative contributions in the massive boson production at high-energy colliders is strongly reduced as compared to Drell-Yan pair production in fixed-target experiments. Nonetheless, this dependence is not entirely negligible at small transverse momenta of W bosons, roughly for $q_T \sim 5$ GeV or less. To give an idea about the typical size of the nonperturbative contributions, Fig. 17 shows the event rate for the single-spin cross section $d\Delta_L\sigma/dp_{T\ell}$ at $\mathcal{L} = 800$ pb^{-1}, integrated over the STAR acceptance range $-1 \leq y_\ell \leq 1$. This rate was calculated using two parameterizations [17, 27] of the nonperturbative part, which were found from the analysis of unpolarized vector boson production. Correspondingly, the resummed cross sections were calculated with the assumption that $S_{NP}|_{single-spin} = S_{NP}|_{unpolarized}$. It can be seen that the sensitivity to the nonperturbative input is small, but, nonetheless, visible near the Jacobian peak. For comparison, we also included the NLO cross section calculated using the phase space slicing method. The NLO curve substantially deviates from the resummation curves, and, moreover, its shape can be drastically modified by varying the phase space slicing parameter q_T^{sep}. In contrast, practically all features of the resummation curve are determined unambiguously by the perturbative contribution, and the remaining small dependence on the nonperturbative contributions is pinned down by utilizing a phenomenological parameterization discussed above. Needless to say, RHIC should explore the spin properties of nonperturbative contributions by studying distributions $d\sigma/dq_T$ in the double-spin γ^* and Z^0 production and $d\sigma/dp_{T\ell}$ in single-spin and double-spin W boson production.

VI. CONCLUSION

Due to the maximal parity violation in the weak current coupling, the longitudinal single-spin asymmetry of W boson production is strongly sensitive to the polarized parton distributions. At the center-of-mass energy of 500 GeV, W boson production events at RHIC can clearly discriminate between various polarized quark luminosities. As a pp collider, RHIC probes the sea quark PDFs in the region of relatively high x, where such PDFs are not adequately constrained even in the unpolarized case. Therefore, RHIC experiments also have a

good potential to reduce the uncertainties in the unpolarized sea quark PDFs in a dedicated study of spin-averaged cross sections.

Since PHENIX and STAR detectors do not determine the missing transverse energy associated with the neutrino from W boson decay, and because the charged leptons from the decay can only be observed in a part of the 4π solid angle, the reconstruction of the asymmetries at the level of W bosons is not easy to realize. As an alternative to the asymmetry $A_L(y_W)$ for the W boson rapidity distribution $d\sigma/dy_W$, we advocate the measurement of the asymmetries $A_L(y_\ell)$ and $A_L(p_{T\ell})$ for the distributions $d\sigma/dy_\ell$ and $d\sigma/dp_{T\ell}$ in the rapidity y_ℓ and transverse momentum $p_{T\ell}$ of the secondary charged lepton. These lepton-level asymmetries can be directly observed at RHIC detectors, they are sizeable, and they can be used to determine the polarized PDFs with high precision.

To reliably predict the distributions of the charged leptons in all available phase space, a theoretical calculation is needed for all-order summation of large logarithmic contributions corresponding to W bosons with a small transverse momentum. At the lepton level, the largest effect of the logarithm resummation is observed in the distributions $d\sigma/dp_{T\ell}$ and $d\Delta_L\sigma/dp_{T\ell}$ in the proximity of the Jacobian peak ($p_{T\ell} \approx M_W/2$). The importance of the resummation can be verified by observing a large difference between the resummed and NLO cross sections near the Jacobian peak, which happens only when the effect of soft gluon radiation is important.

In this paper, we apply the state-of-art resummation calculation [12] for spin-dependent vector boson production to predict reliably the distributions of the observed leptons from W boson decay. In addition to the spin-averaged and single-spin cross sections, we presented a detailed study of single-spin asymmetries for the decay lepton in the presence of kinematical cuts imposed by PHENIX and STAR detectors. Furthermore, we propose to study the distribution $d\Delta_L\sigma/dp_{T\ell}$ at $p_{T\ell} \approx M_W/2$ to learn about the spin (in)dependence of nonperturbative contributions in the CSS resummation formalism. The study of such contributions for different beam polarizations and bosons of different types (γ^*,$W^\pm$, Z^0) will shed light on basic properties of QCD factorization and provide important clues about the nature of the intrinsic transverse motion of partons inside the proton.

Acknowledgments

Authors would like to thank C. Balazs, D. Boer, G. Bunce, M. Grosse Perdekamp, S. Gupta, J. Kiryluk, N. Saito, M. Stratmann, W. Vogelsang, and members of the CTEQ collaboration for helpful discussions. We are grateful to F. Olness for his comments on the manuscript. We thank the organizers of RHIC Spin workshops, where preliminary results of this work were presented. The work of P. M. N. has been supported by the U.S. Department of Energy and Lightner-Sams Foundation. The research of C. P. Y. has been supported by the National Science Foundation under grant PHY-0100677.

---

[1] G. Bunce, N. Saito, J. Soffer, and W. Vogelsang, Ann. Rev. Nucl. Part. Sci. **50**, 525 (2000).

[2] C. Bourrely and J. Soffer, Nucl. Phys. **B423**, 329 (1994).

[3] C. Bourrely and J. Soffer, Nucl. Phys. **B445**, 341 (1995).

[4] P. M. Nadolsky (1995), hep-ph/9503419.

[5] L. C. Bland (STAR Collaboration) (2000), hep-ex/0002061.

[6] D. P. Morrison et al. (PHENIX Collaboration), Nucl. Phys. **A638**, 565 (1998).

[7] J. W. Harris (STAR Collaboration), Nucl. Phys. **A566**, 277c (1994).

[8] T. Affolder et al. (CDF Collaboration), Phys. Rev. **D64**, 052001 (2001).

[9] V. M. Abazov et al. (D0 Collaboration), Phys. Rev. **D66**, 012001 (2002).

[10] J. C. Collins, D. E. Soper, and G. Sterman, Nucl. Phys. **B250**, 199 (1985).

[11] C. Balazs and C.-P. Yuan, Phys. Rev. **D56**, 5558 (1997).

[12] P. M. Nadolsky and C.-P. Yuan (2003), hep-ph/0304001.

[13] A. Weber, Nucl. Phys. **B403**, 545 (1993).

[14] R. Mertig and W. L. van Neerven, Z. Phys. **C70**, 637 (1996).

[15] W. Vogelsang, Phys. Rev. **D54**, 2023 (1996).

[16] W. Vogelsang, Nucl. Phys. **B475**, 47 (1996).

[17] F. Landry, R. Brock, P. M. Nadolsky, and C. P. Yuan (2002), hep-ph/0212159.

[18] J. Pumplin et al., JHEP **07**, 012 (2002), hep-ph/0201195.

[19] D. Stump et al. (2003), hep-ph/0303013.

[20] H. L. Lai et al. (CTEQ Collaboration), Eur. Phys. J. **C12**, 375 (2000).

[21] M. Gluck, E. Reya, M. Stratmann, and W. Vogelsang, Phys. Rev. **D63**, 094005 (2001).

[22] T. Gehrmann, Nucl. Phys. **B534**, 21 (1998).

[23] T. Gehrmann and W. J. Stirling, Phys. Rev. **D53**, 6100 (1996).

[24] M. Gluck, E. Reya, M. Stratmann, and W. Vogelsang, Phys. Rev. **D53**, 4775 (1996).

[25] C. T. H. Davies, B. R. Webber, and W. J. Stirling, Nucl. Phys. **B256**, 413 (1985).

[26] P. B. Arnold and R. P. Kauffman, Nucl. Phys. **B349**, 381 (1991).

[27] G. A. Ladinsky and C.-P. Yuan, Phys. Rev. **D50**, 4239 (1994).

Table I: The unpolarized cross sections (in pb) and numbers of events N for the processes $pp \to (W^{\pm} \to \ell\nu_\ell)X$ and $pp \to (Z^0 \to \ell\bar{\ell})X$ at RHIC. Here ℓ and ν_ℓ are leptons of one lepton generation, and the decay branching ratios were calculated to be $\mathrm{Br}\,(W^{\pm} \to \ell\nu_\ell) = 0.11$, $\mathrm{Br}\left(Z^0 \to \ell\bar{\ell}\right) = 0.034$. The numbers in parentheses show the relative uncertainties. Also shown are the Born-level momentum fractions $x = Q/\sqrt{s}$ corresponding to $y_W = 0$ (or $y_Z = 0$). The uncertainties $\delta\sigma_{PDF}$ in the cross sections σ are due to the uncertainties in the parton distribution functions estimated according to the CTEQ6 analysis [18, 19]. The uncertainties in N are purely statistical.

		$\sqrt{s} = 200$ GeV $\mathcal{L} = 320$ pb^{-1}	$\sqrt{s} = 500$GeV $\mathcal{L} = 800$ pb^{-1}
W^+	$x\vert_{y_W=0}$	0.4	0.16
	$\sigma \pm \delta\sigma_{PDF}\left(\frac{\delta\sigma_{PDF}}{\sigma}\right)$	$1.38 \pm 0.34\,(0.25)$	$124 \pm 9\,(0.07)$
	$N \pm \sqrt{N}(1/\sqrt{N})$	$440 \pm 20\,(0.05)$	$99200 \pm 300\,(0.003)$
W^-	$x\vert_{y_W=0}$	0.4	0.16
	$\sigma \pm \delta\sigma_{PDF}\left(\frac{\delta\sigma_{PDF}}{\sigma}\right)$	$0.43 \pm 0.12\,(0.27)$	$41 \pm 4\,(0.10)$
	$N \pm \sqrt{N}(1/\sqrt{N})$	$142 \pm 12\,(0.09)$	$32800 \pm 200\,(0.006)$
Z^0	$x\vert_{y_Z=0}$	0.46	0.18
	$\sigma \pm \delta\sigma_{PDF}\left(\frac{\delta\sigma_{PDF}}{\sigma}\right)$	$0.07 \pm 0.02\,(0.26)$	$10.0 \pm 0.8\,(0.08)$
	$N \pm \sqrt{N}(1/\sqrt{N})$	$21 \pm 5\,(0.22)$	$8010 \pm 90\,(0.01)$

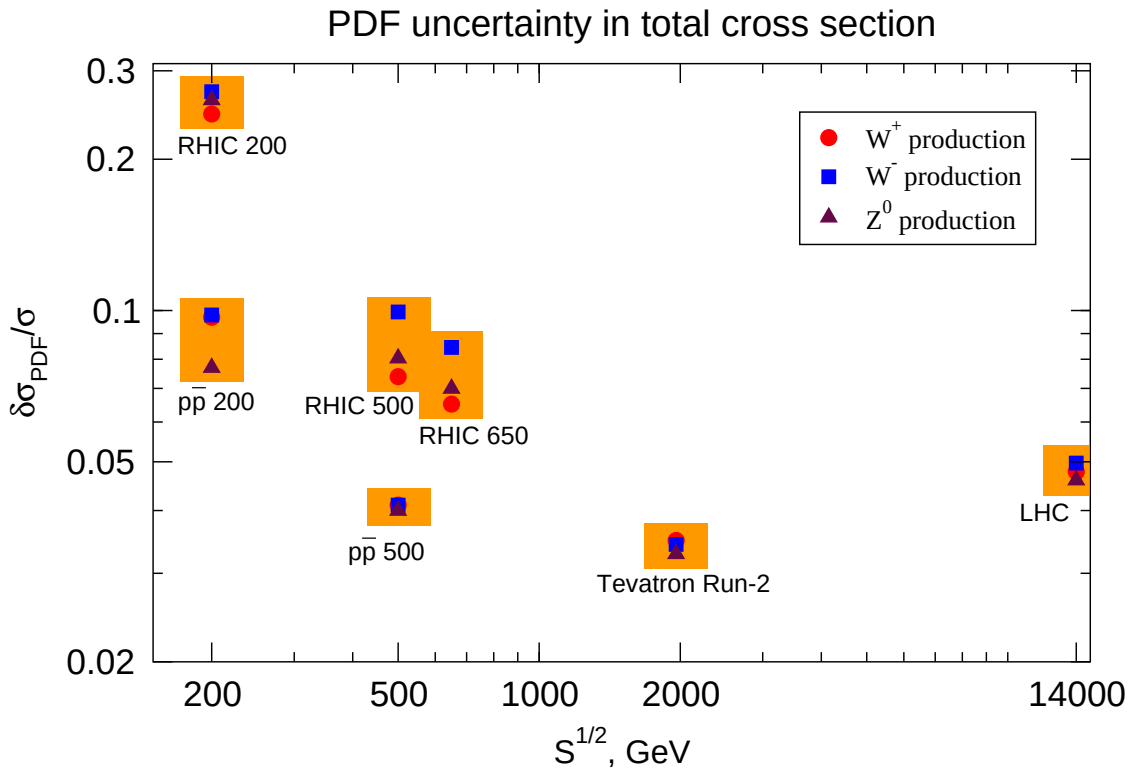

Figure 1: Uncertainties due to the PDF errors in the unpolarized cross sections of W and Z^0 boson production at various colliders. The shown uncertainties are for RHIC at $\sqrt{s} = 200$, 500, and 650 GeV; Tevatron Run-2; LHC; and fictitious $p\bar{p}$ colliders at $\sqrt{s} = 200$ and 500 GeV.

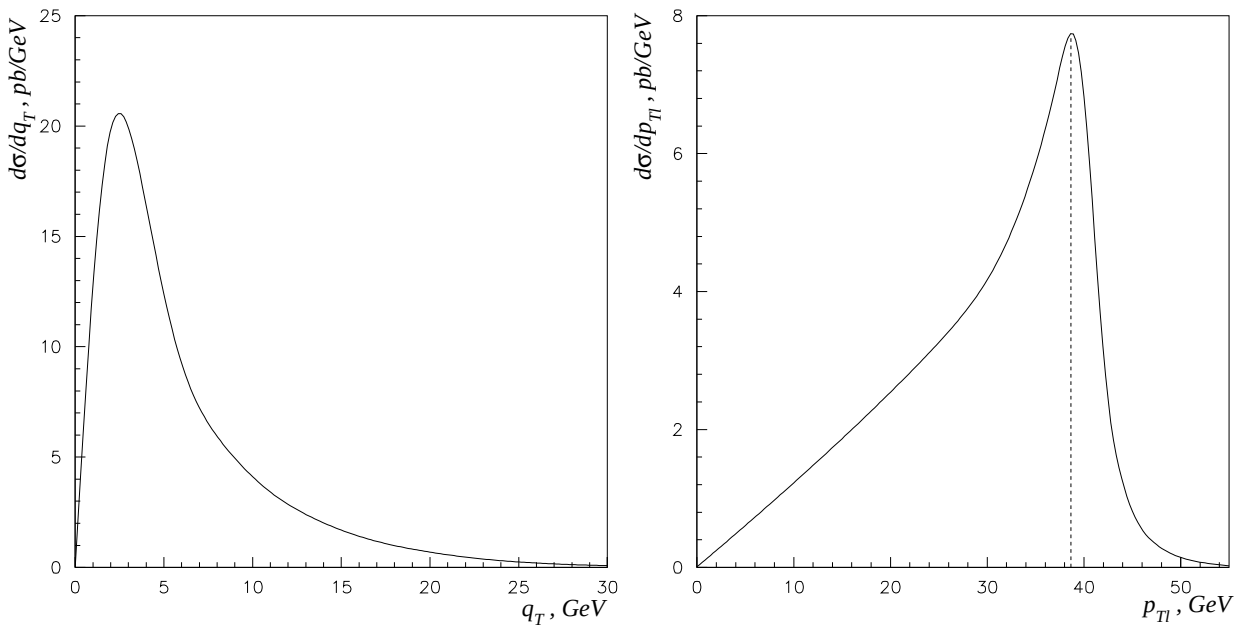

(a) (b)

Figure 2: The unpolarized cross section for the process $pp \to (W^+ \to \ell^+ \nu_\ell) X$ at $\sqrt{s} = 500$ GeV as a function of (a) the transverse momentum q_T of the W^+ boson and (b) the transverse momentum $p_{T\ell}$ of the charged lepton, as predicted by the resummation calculation. CTEQ5M PDFs [20] were used.

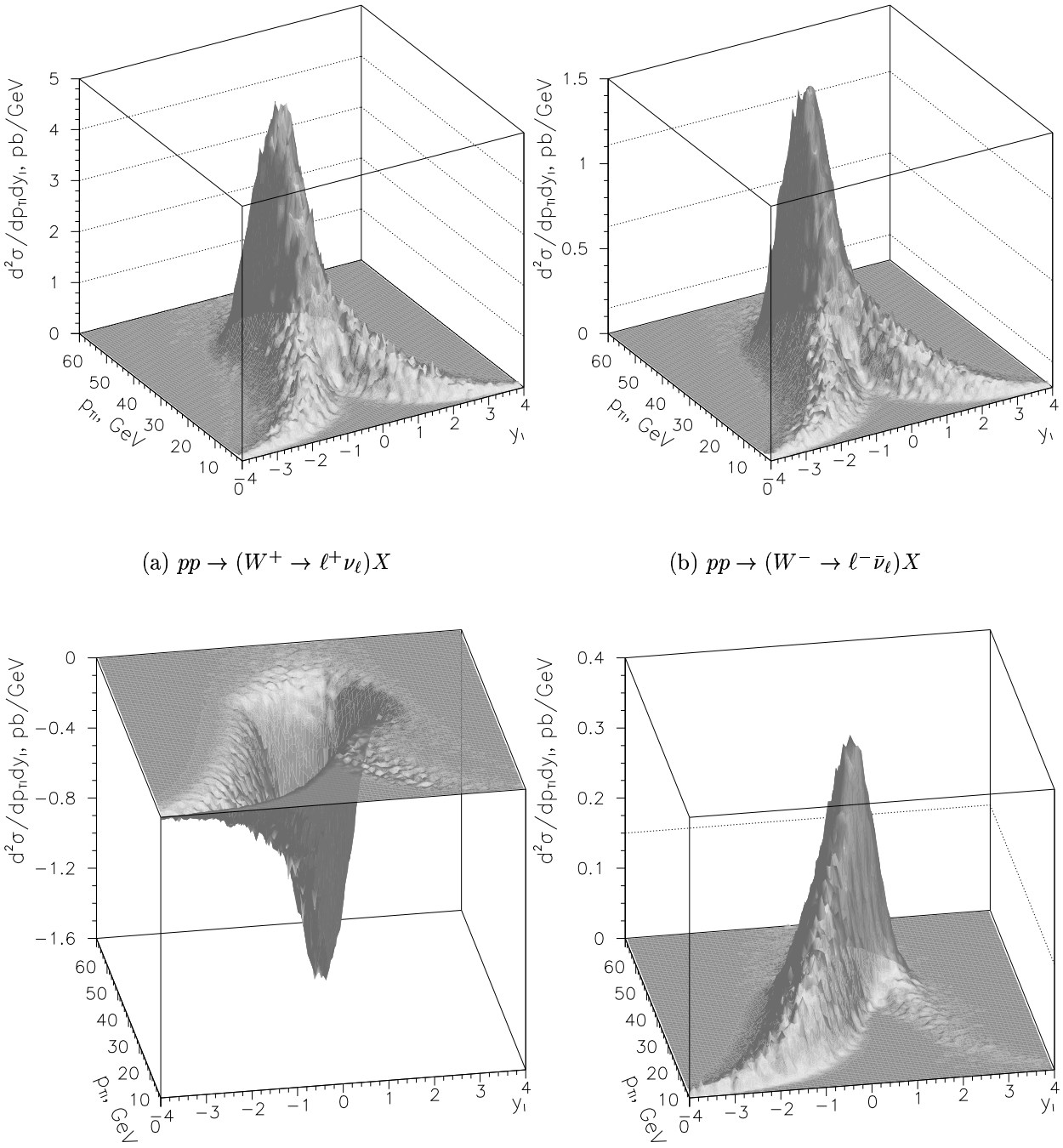

(a) $pp \to (W^+ \to \ell^+\nu_\ell)X$

(b) $pp \to (W^- \to \ell^-\bar{\nu}_\ell)X$

(c) $\Delta_L pp \to (W^+ \to \ell^+\nu_\ell)X$

(d) $\Delta_L pp \to (W^- \to \ell^-\bar{\nu}_\ell)X$

Figure 3: Resummed two-variable distributions $d^2\sigma/dp_{T\ell}dy_\ell$ for (a), (b) unpolarized and (c), (d) single-spin cross sections in W^+ and W^- boson production. The unpolarized and single-spin cross sections are calculated using CTEQ5M [20] and GRSV-2000 [21] standard PDF sets, respectively.

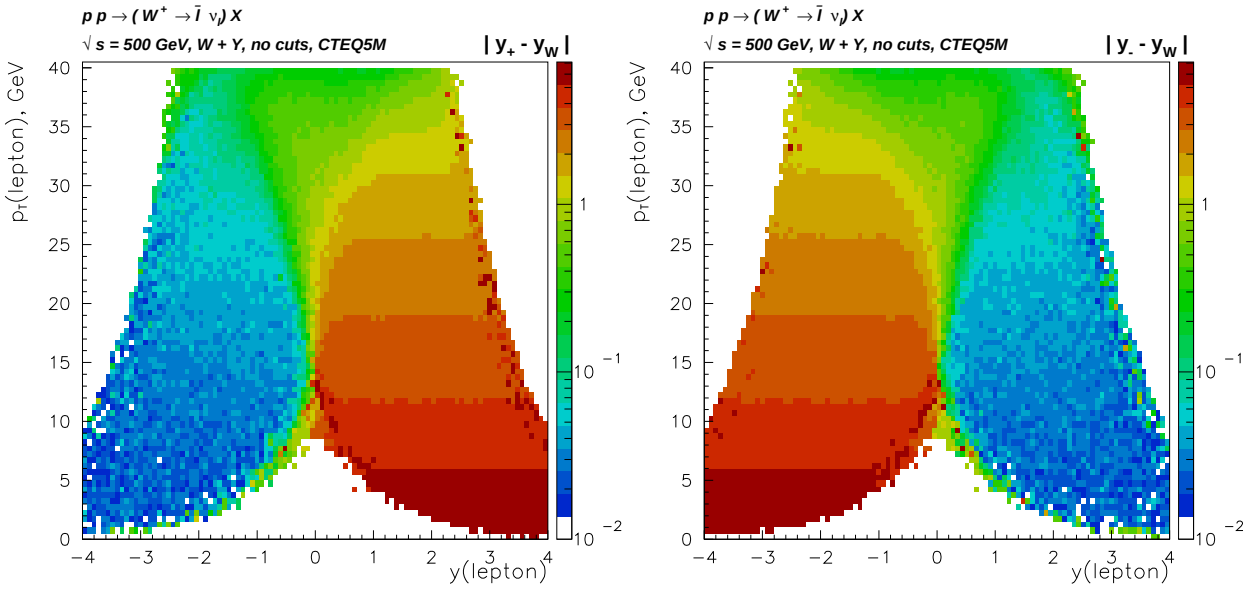

(a) (b)

Figure 4: The average differences between the exact value of y_W and two approximate solutions $y_\pm$ of Eqs. (10)-(13) as a function of the charged lepton's rapidity y_ℓ and transverse momentum $p_{T\ell}$. The resummation calculation and CTEQ5M PDFs [20] were used. The color corresponds to the magnitude of $|y_\pm - y_W|$ according to the scales on the right-hand side of the plots. The white color corresponds to the regions with no event rate. According to the figure, the solutions y_+ and y_- provide good approximations in the limits $y_\ell \ll 0$ and $y_\ell \gg 0$, respectively.

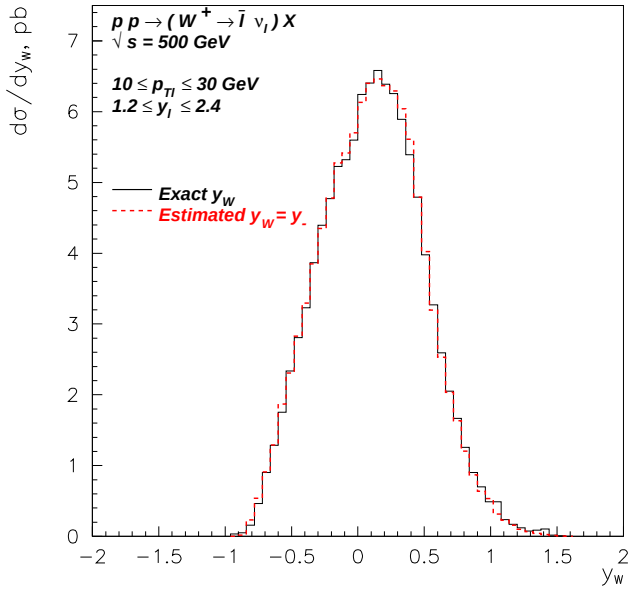

Figure 5: Comparison of the distributions $d\sigma/dy_-$ and $d\sigma/dy_W$ in the region of the validity of the approximate solution y_-, as predicted by the resummation calculation. The constraints $1.2 \leq y_\ell \leq 2.4$ and $p_{T\ell} \geq 10$ GeV imitate kinematical cuts for a measurement with the PHENIX muon detector. The cut $p_{T\ell} \leq 30$ GeV suppresses contributions with large deviations of y_- from y_W (cf. Fig. 4(b)). CTEQ5M PDFs [20] were used.

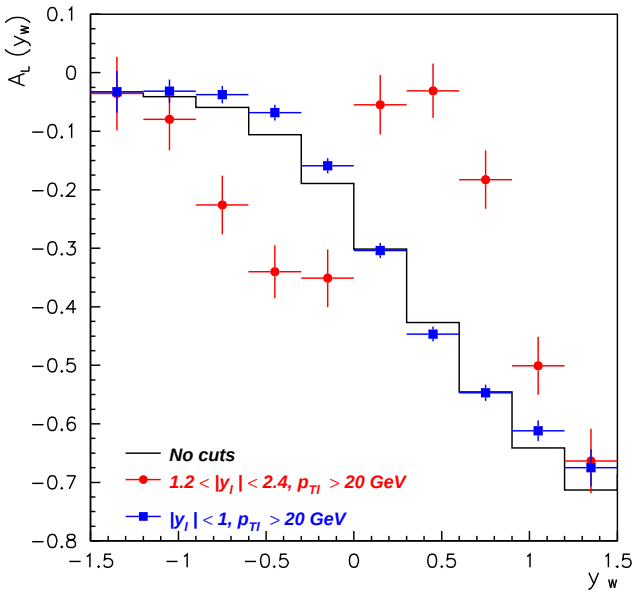

Figure 6: Dependence of the asymmetry $A_L(y_W)$ on the cuts imposed on the momentum of the observed charged lepton in the process $\Delta_L pp \to (W^+ \to \ell^+ \nu_\ell) X$, as predicted by the resummation calculation. The GRSV-2000 standard set [21] of the polarized PDFs was used. The projected statistical errors in $A_L(y_W)$ (shown by error bars) are estimated with the help of Eq. (7) for the bin sizes shown in the figure.

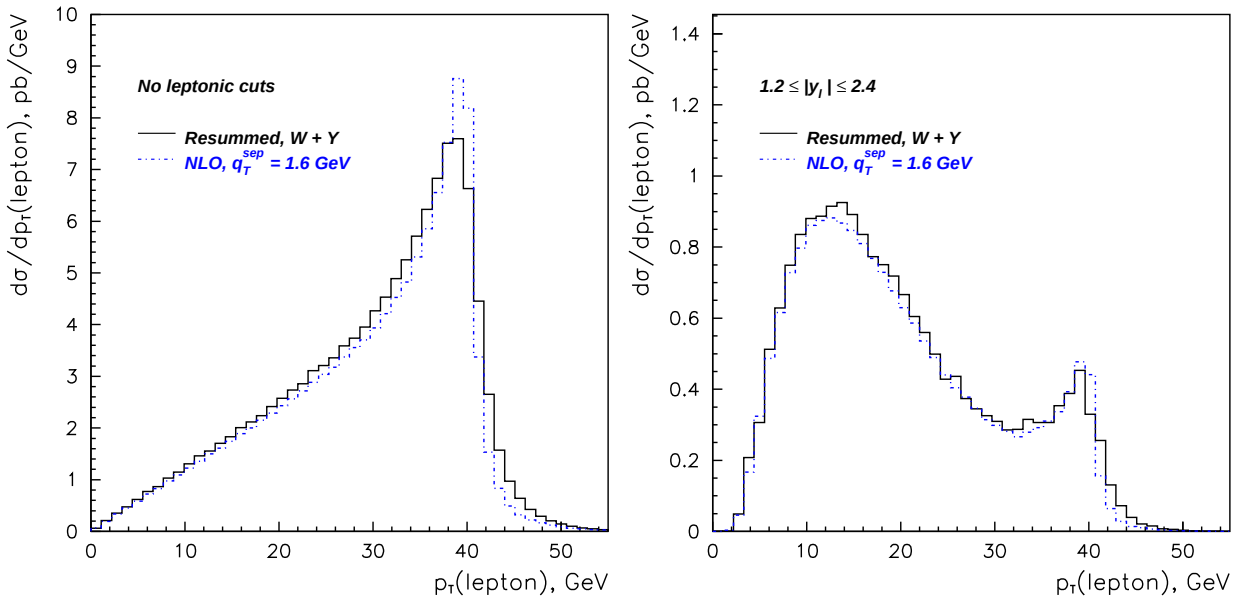

(a) No cuts

(b) $1.2 \le |y_\ell| \le 2.4$

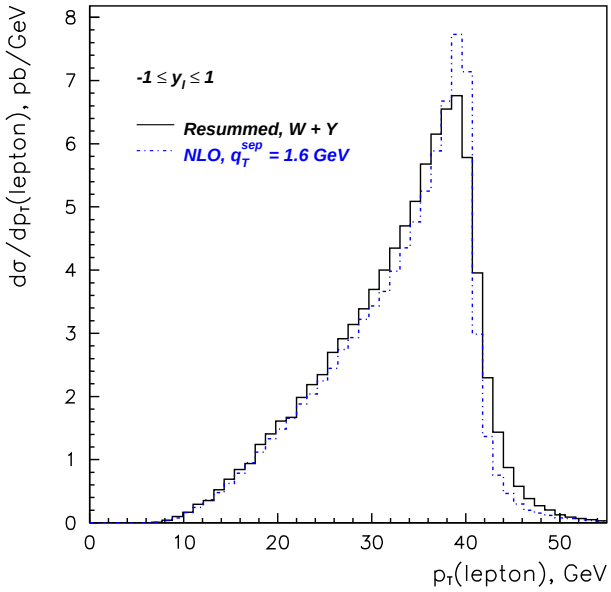

(c) $-1 \le y_\ell \le 1$

Figure 7: Unpolarized resummed (solid) and NLO (dashed) cross sections $d\sigma/dp_{T\ell}$ in the process $pp \to (W^+ \to \ell^+\nu_\ell)X$ for various cuts on the lepton's rapidity. CTEQ5M PDFs [20] were used.

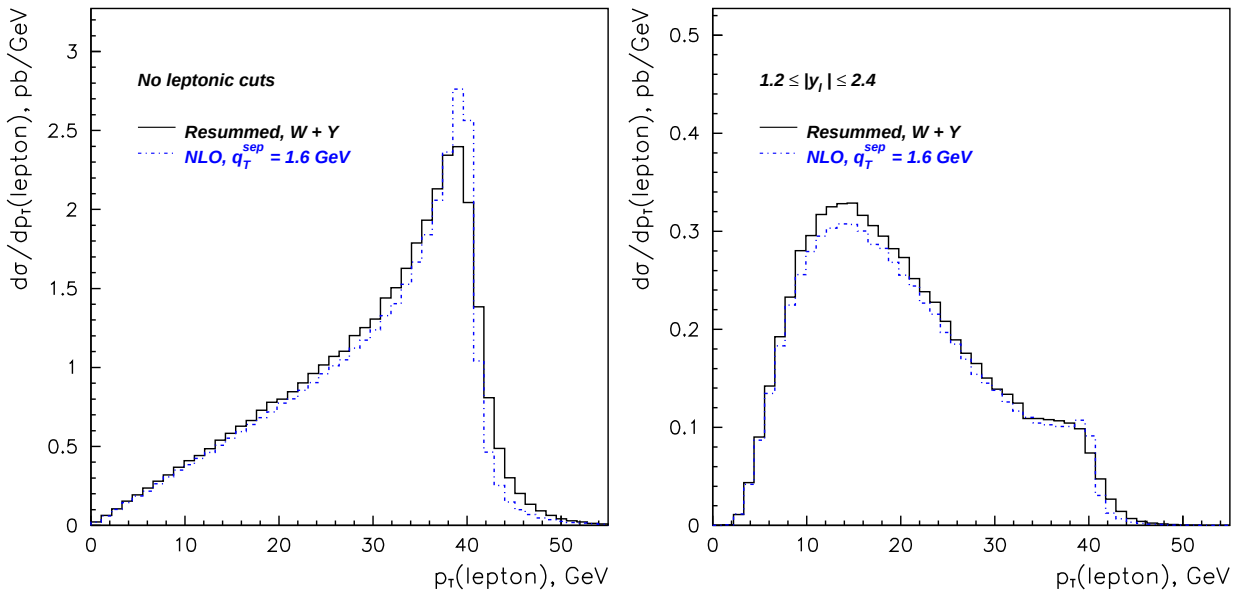

(a) No cuts

(b) $1.2 \le |y_\ell| \le 2.4$

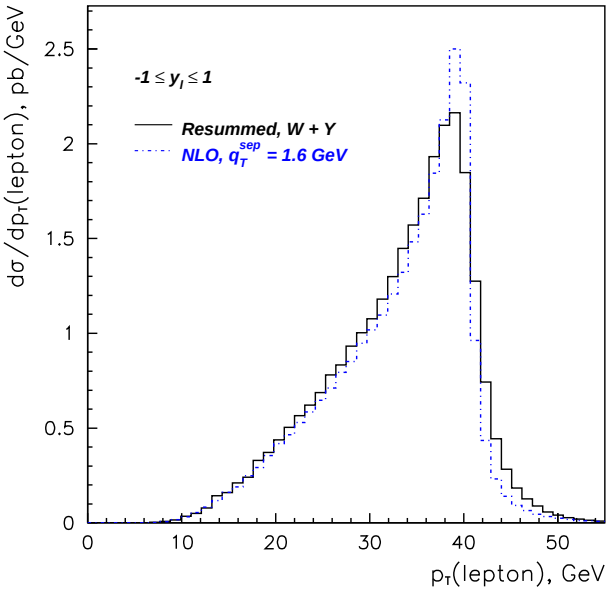

(c) $-1 \le y_\ell \le 1$

Figure 8: Unpolarized resummed (solid) and NLO (dashed) cross sections $d\sigma/dp_{T\ell}$ in the process $pp \to (W^- \to \ell^- \bar{\nu}_\ell)X$ for various cuts on the lepton's rapidity. CTEQ5M PDFs [20] were used.

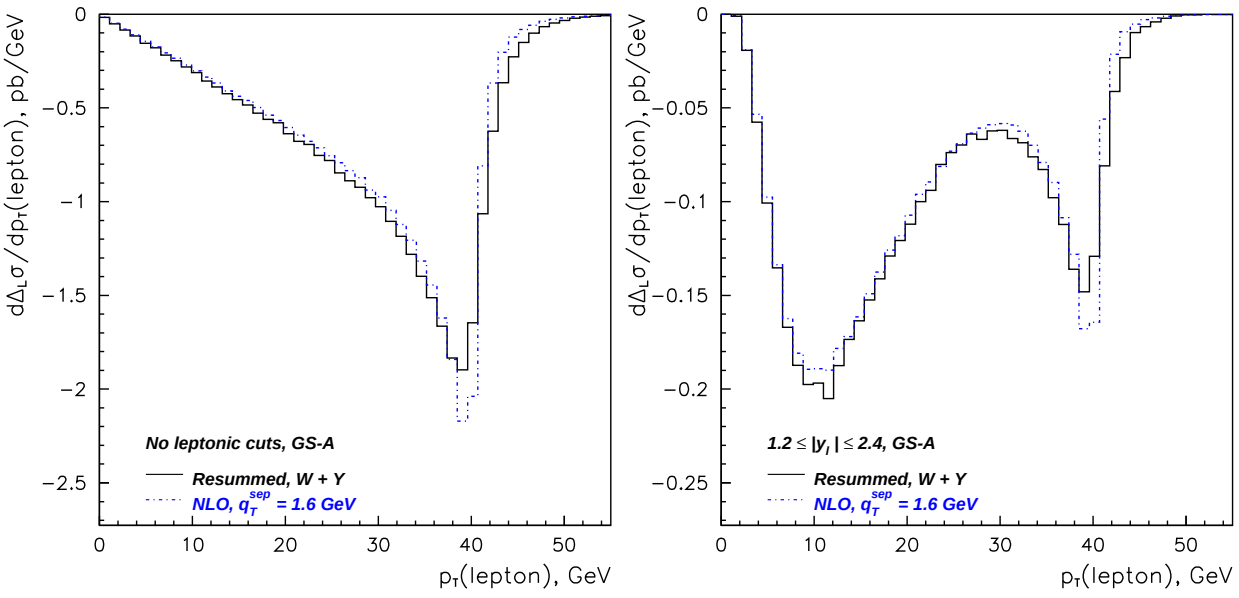

(a) No cuts

(b) $1.2 \leq |y_\ell| \leq 2.4$

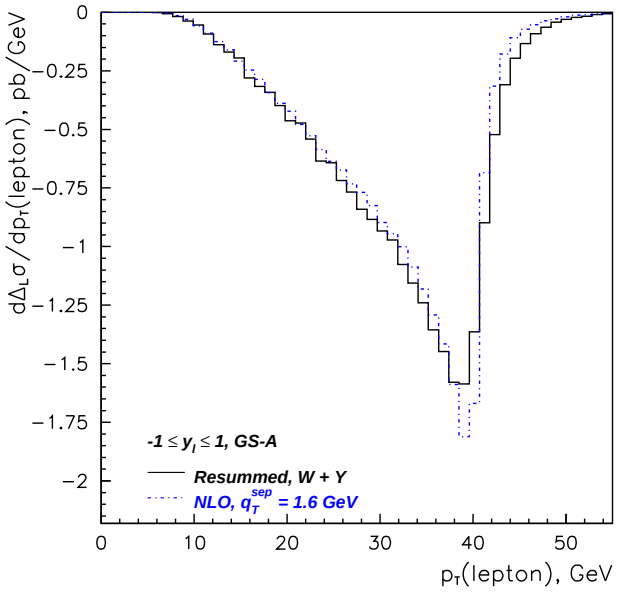

(c) $-1 \leq y_\ell \leq 1$

Figure 9: Single-spin resummed (solid) and NLO (dashed) cross sections $d\Delta_L\sigma/dp_{T\ell}$ in the process $\Delta_L pp \to (W^+ \to \ell^+\nu_\ell)X$ for various cuts on the lepton's rapidity. Gehrmann-Stirling PDF set A [23] were used.

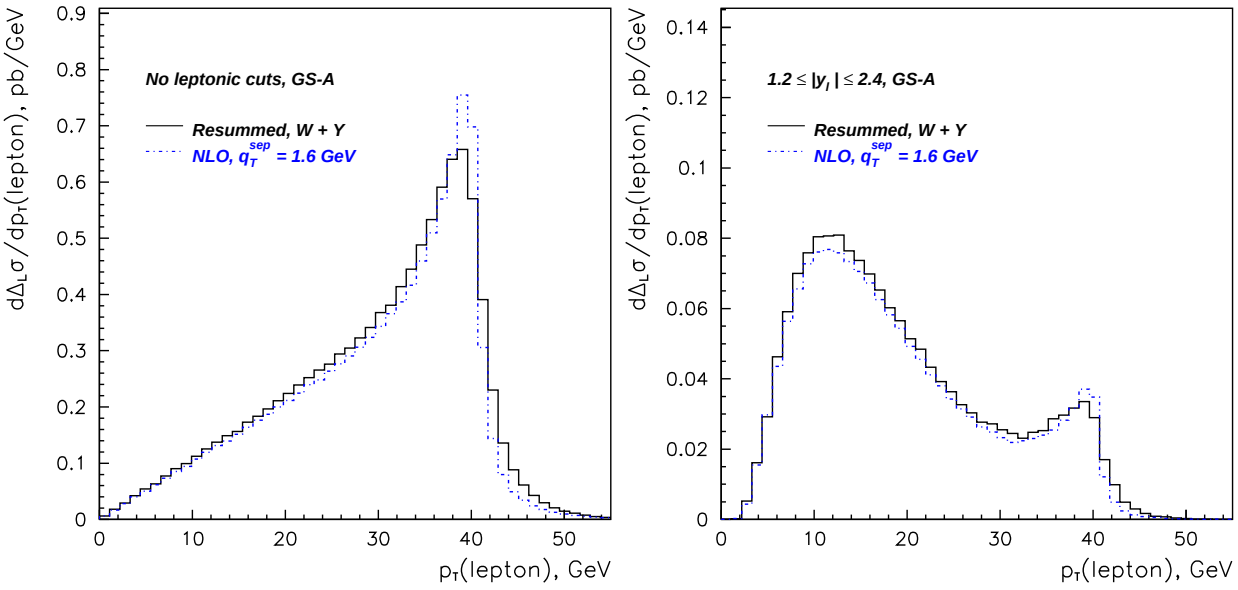

(a) No cuts

(b) $1.2 \leq |y_\ell| \leq 2.4$

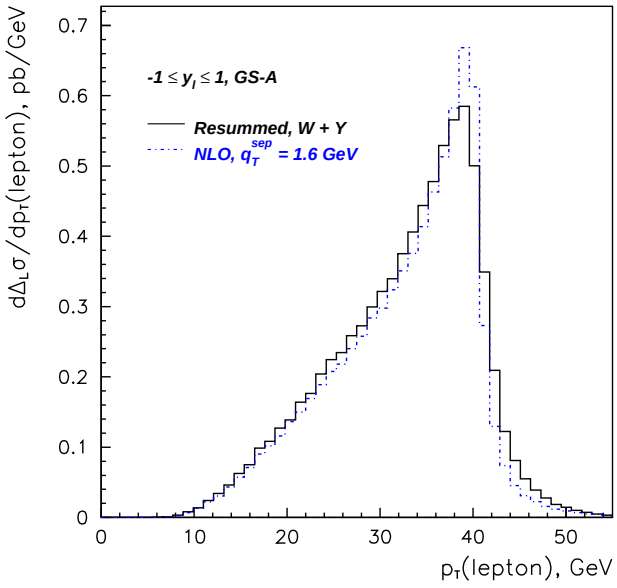

(c) $-1 \leq y_\ell \leq 1$

Figure 10: Single-spin resummed (solid) and NLO (dashed) cross sections $d\Delta_L\sigma/dp_{T\ell}$ in the process $\Delta_L pp \to (W^- \to \ell^-\bar{\nu}_\ell)X$ for various cuts on the lepton's rapidity. Gehrmann-Stirling PDF set A [23] was used.

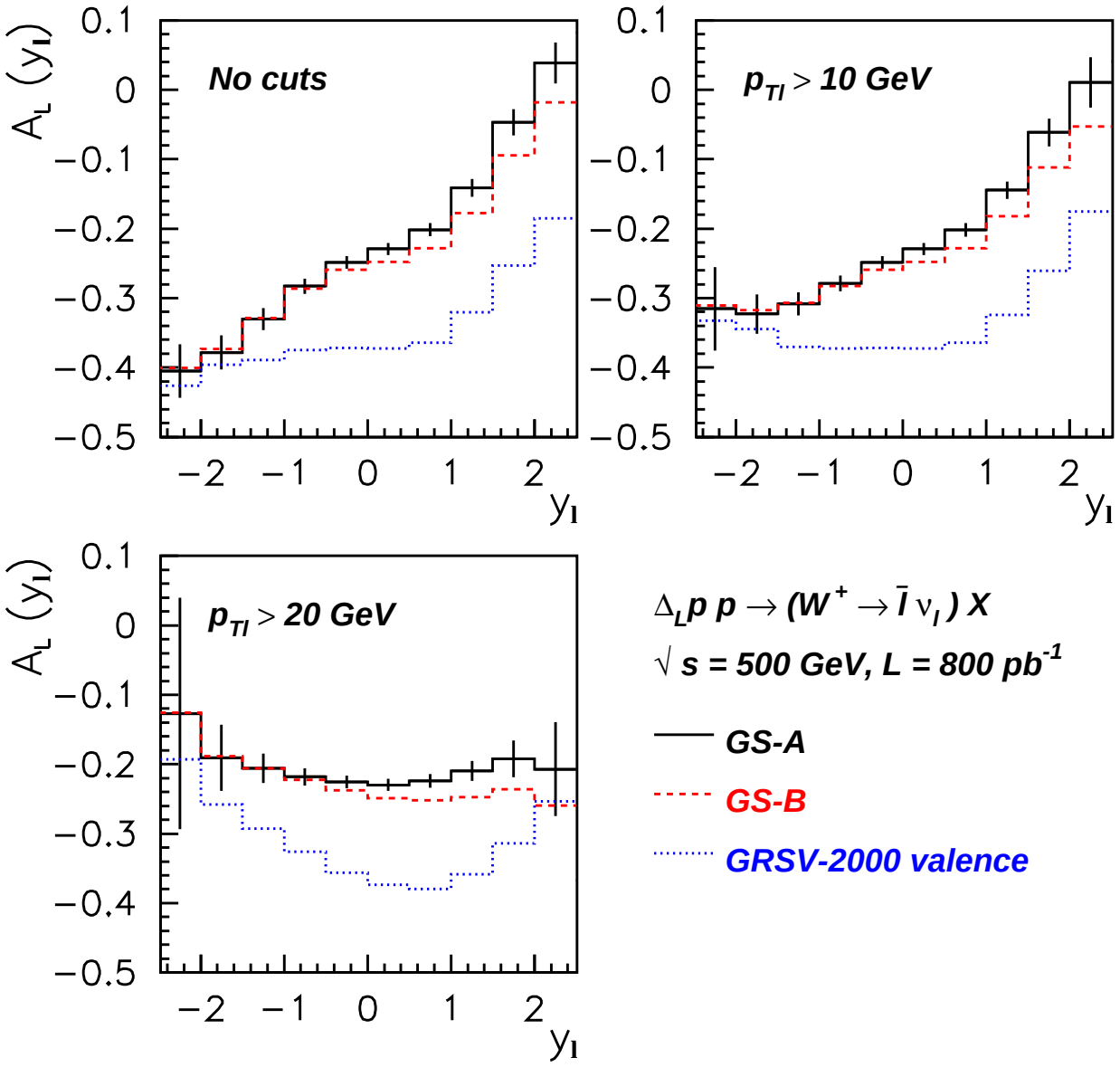

Figure 11: Asymmetries $A_L(y_\ell)$ for various selection cuts on $p_{T\ell}$ in W^+ boson production, as predicted by the resummation calculation. The asymmetry is shown for the Gehrmann-Stirling PDF sets A (solid) and B (dashed), as well as for the GRSV valence-like PDF set (dotted).

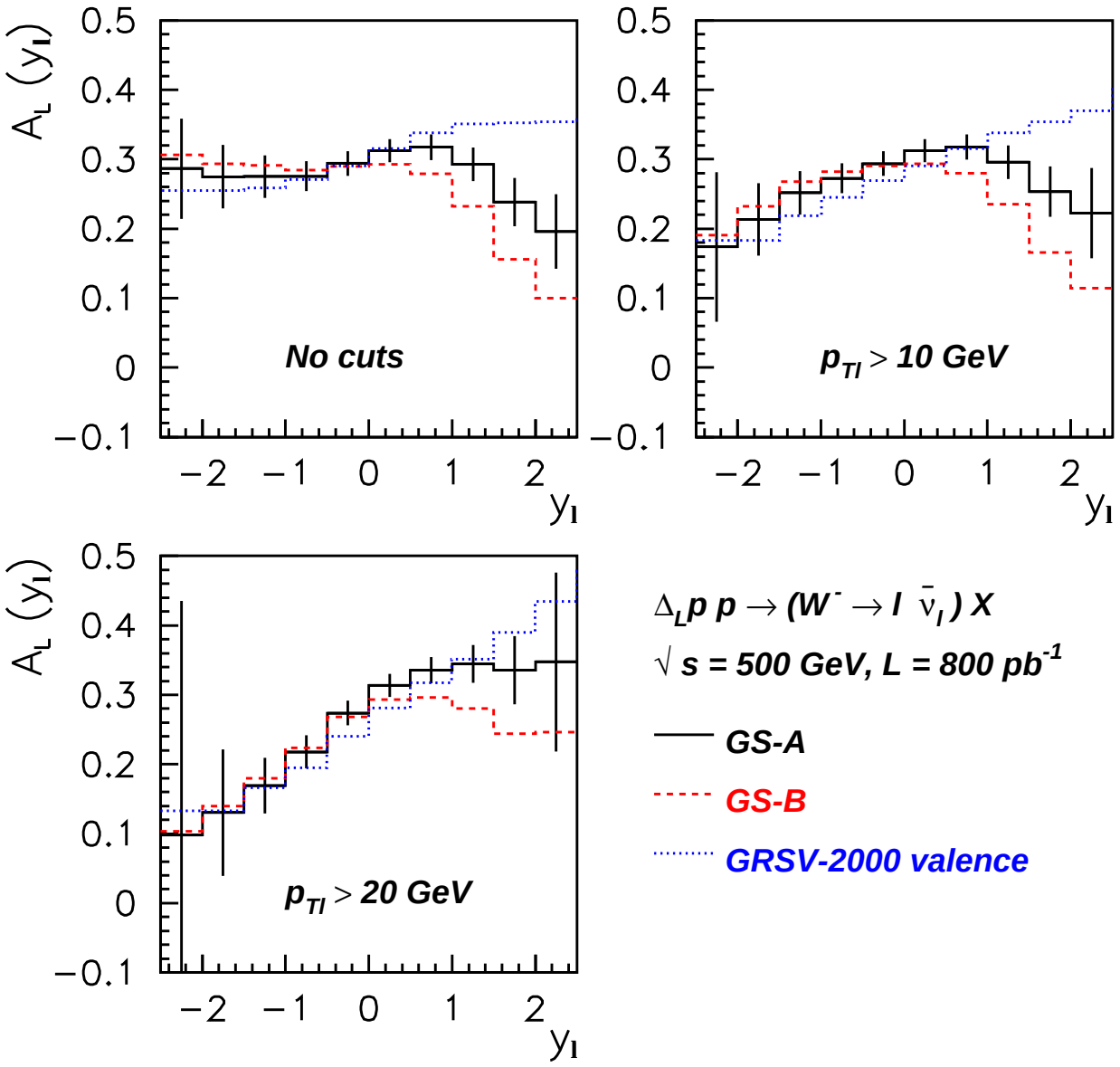

Figure 12: Asymmetries $A_L(y_\ell)$ for various selection cuts on $p_{T\ell}$ in W^- boson production, as predicted by the resummation calculation. The asymmetry is shown for the Gehrmann-Stirling PDF sets A (solid) and B (dashed), as well as for the GRSV valence-like PDF set (dotted).

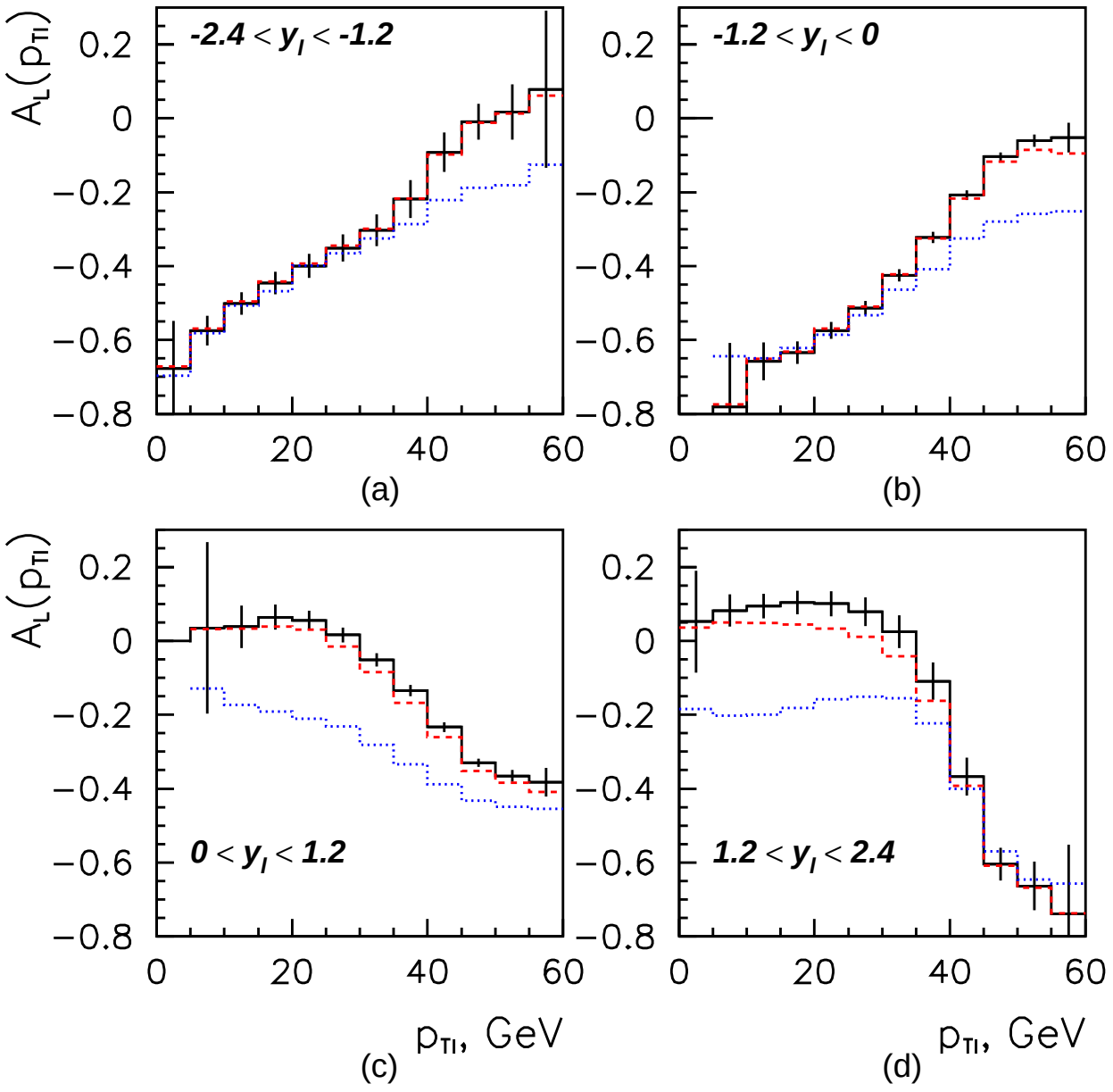

Figure 13: Asymmetries $A_L(p_{T\ell})$ for various selection cuts on y_ℓ in W^+ boson production, as predicted by the resummation calculation. The asymmetry is shown for the Gehrmann-Stirling PDF sets A (solid) and B (dashed), as well as for the GRSV valence-like PDF set (dotted).

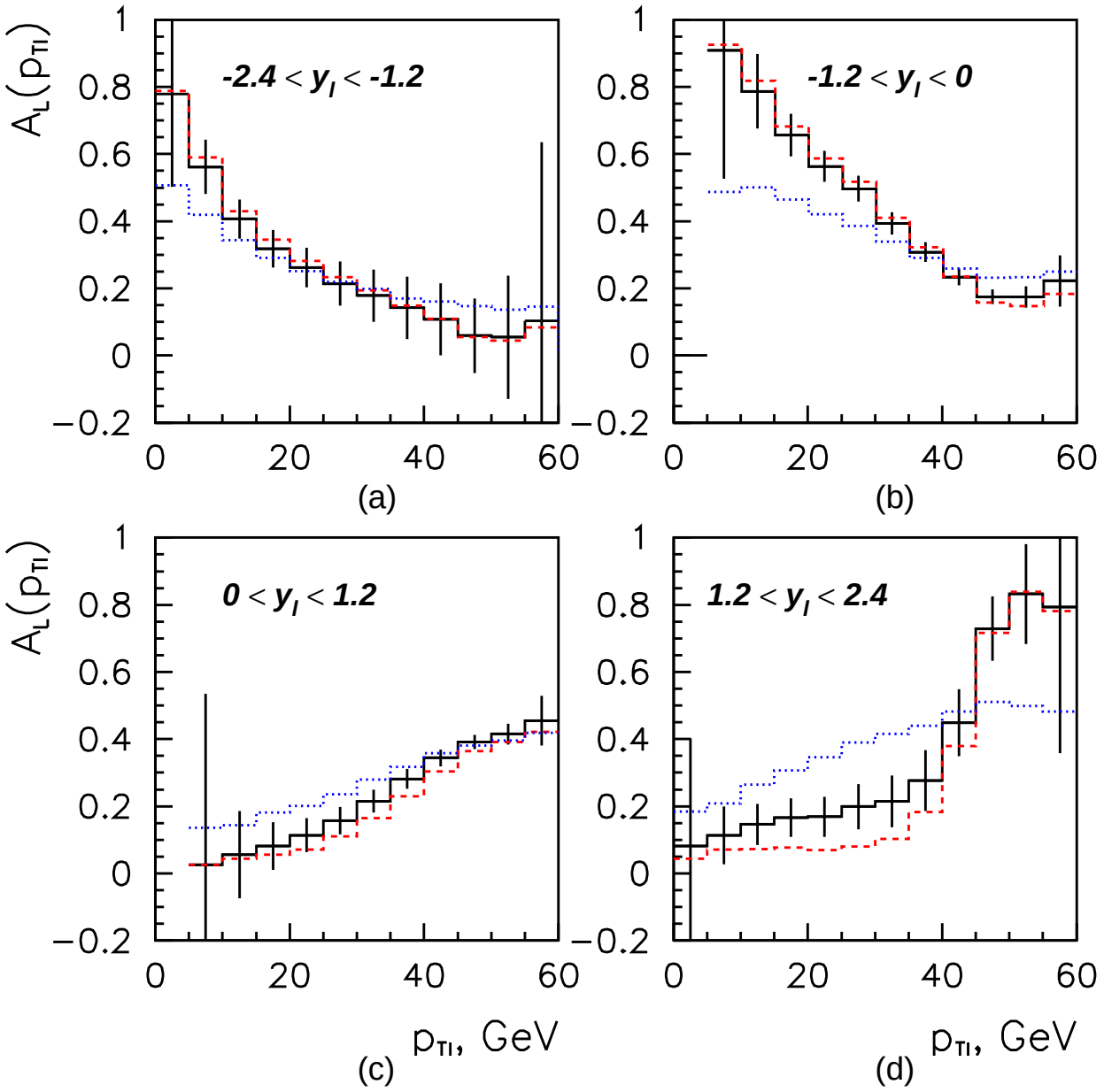

Figure 14: Asymmetries $A_L(p_{T\ell})$ for various selection cuts on y_ℓ in W^- boson production, as predicted by the resummation calculation. The asymmetry is shown for the Gehrmann-Stirling PDF sets A (solid) and B (dashed), as well as for the GRSV valence-like PDF set (dotted).

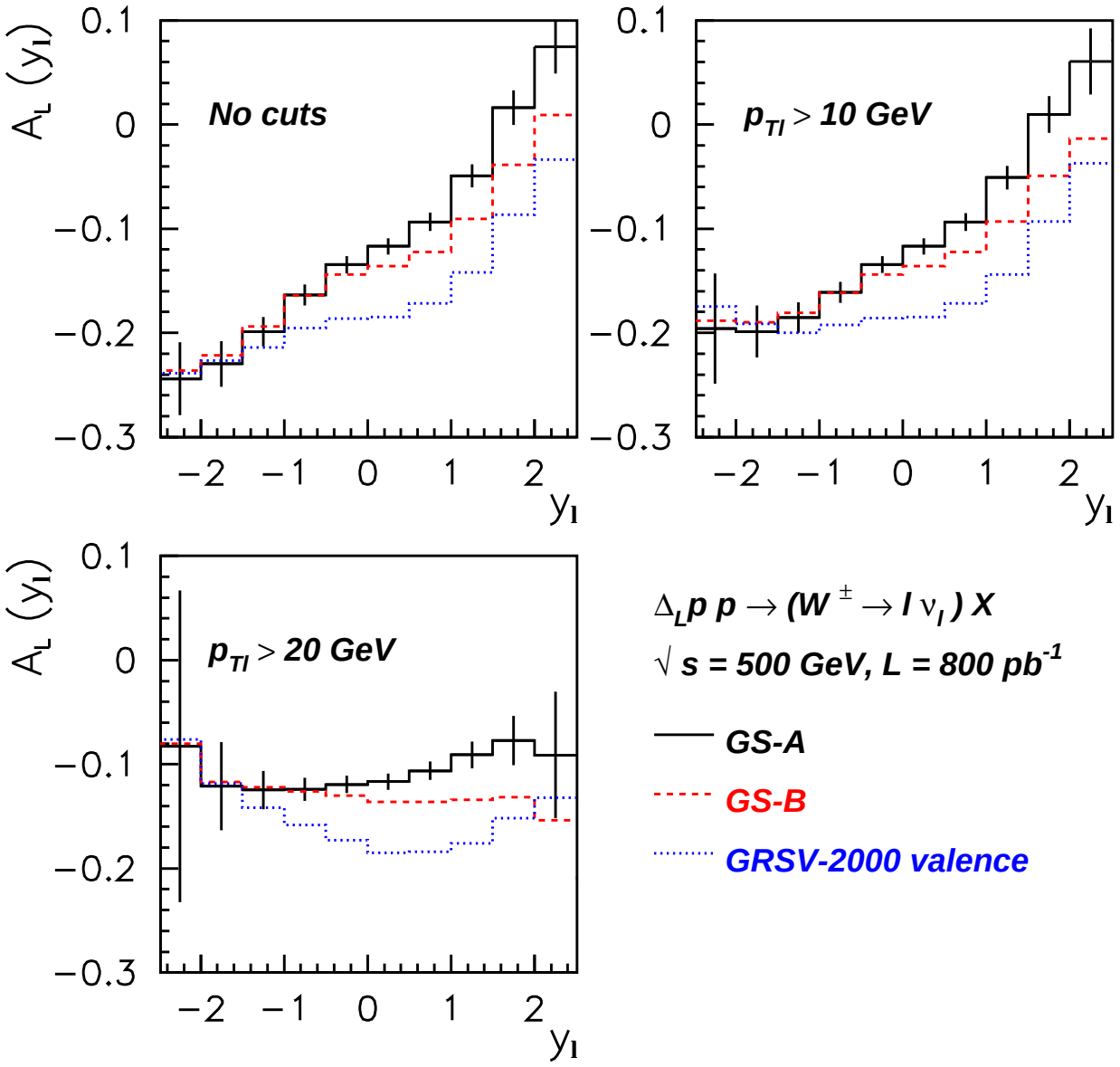

Figure 15: Asymmetries $A_L(y_\ell)$ for various selection cuts on $p_{T\ell}$ for the combined sample of W^+ and W^- bosons, as predicted by the resummation calculation. The asymmetry is shown for the Gehrmann-Stirling PDF sets A (solid) and B (dashed), as well as for the GRSV valence-like PDF set (dotted).

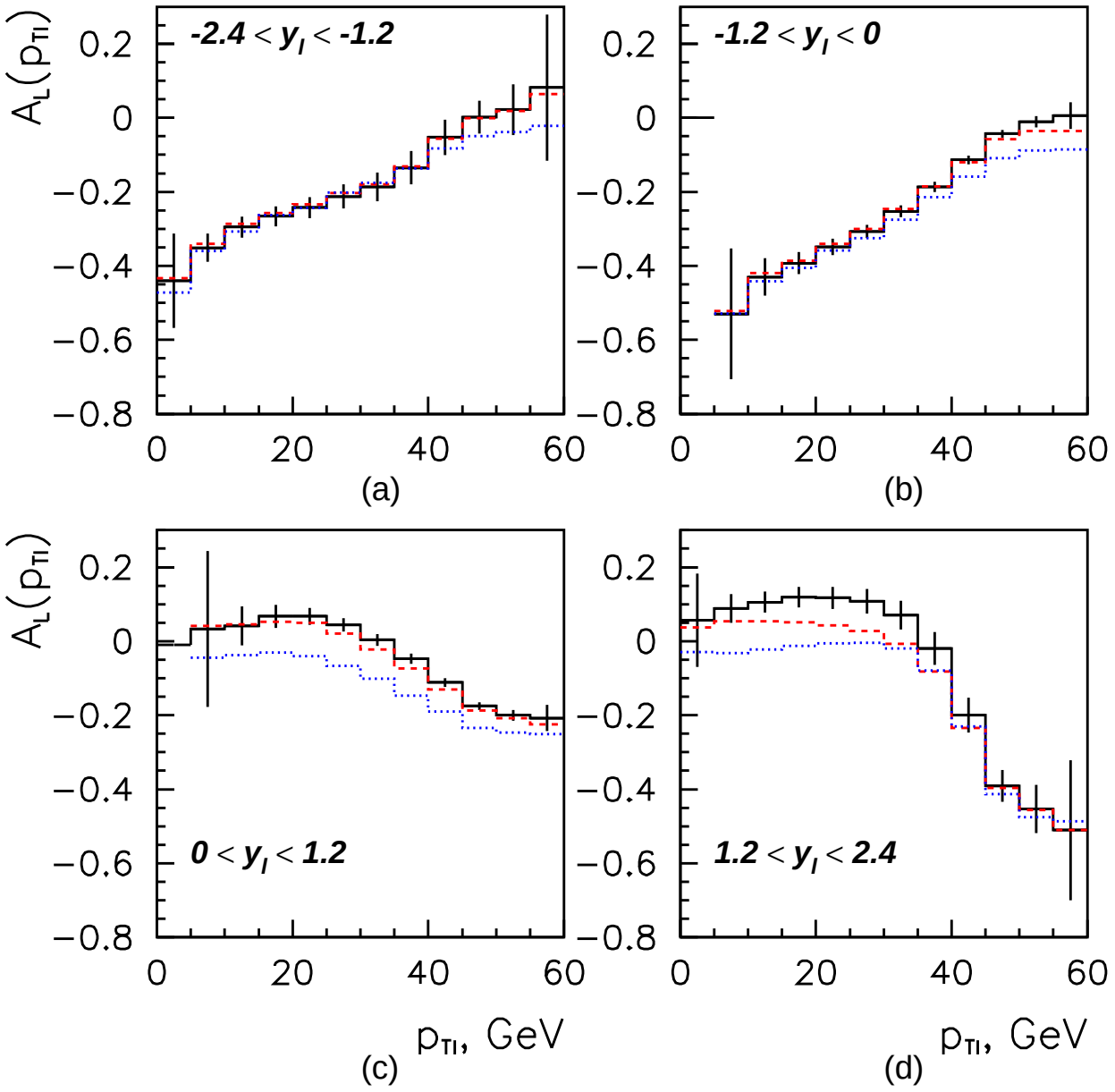

Figure 16: Asymmetries $A_L(p_{T\ell})$ for various selection cuts on y_ℓ for the combined sample of W^+ and W^- bosons, as predicted by the resummation calculation. The asymmetry is shown for the Gehrmann-Stirling PDF sets A (solid) and B (dashed), as well as for the GRSV valence-like PDF set (dotted).

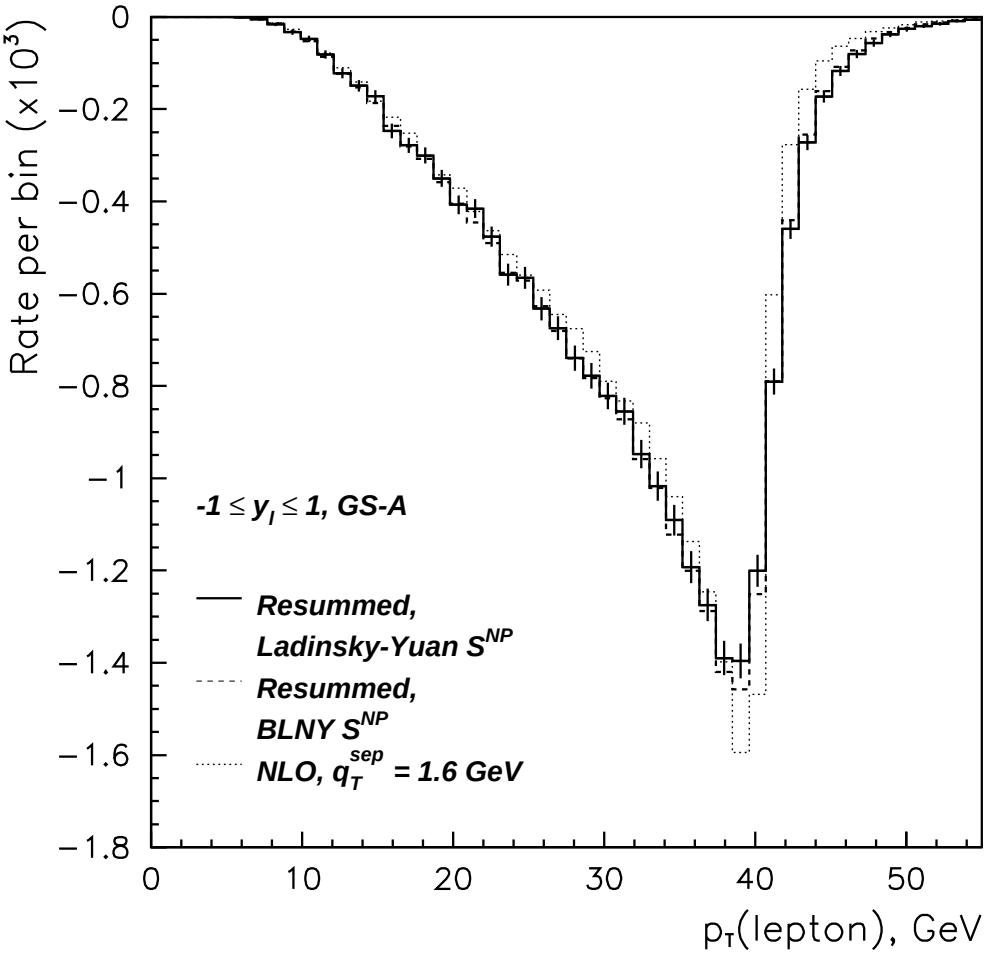

Figure 17: The single-spin charged lepton transverse momentum distribution $d\Delta_L\sigma/dp_{T\ell}$ for W^+ boson production discussed in the main text. The nonperturbative parts of the resummed cross sections were approximated by the Ladinsky-Yuan [27] (solid) and Brock-Landry-Nadolsky-Yuan [17] (dashed) phenomenological parameterizations from unpolarized vector boson production. The NLO cross section is shown for comparison as a dotted line. The distributions are calculated using the Gehrmann-Stirling PDF set A [23].